

**CHARACTERIZATION OF THE 3-D PROPERTIES OF THE FINE-
GRAINED TURBIDITE 8 SAND RESERVOIR, GREEN CANYON
18, GULF OF MEXICO**

A Thesis

by

MATTHIEU PLANTEVIN

Submitted to the Office of Graduate Studies of
Texas A&M University
in partial fulfillment of the requirements for the degree of

MASTER OF SCIENCE

May 2002

Major subject: Geology

CHARACTERIZATION OF THE 3-D PROPERTIES OF THE FINE-
GRAINED TURBIDITE & SAND RESERVOIR, GREEN CANYON 18,
GULF OF MEXICO

A Thesis

by

MATTHIEU PLANTEVIN

Submitted to Texas A&M University
in partial fulfillment of the requirements
for the degree of

MASTER OF SCIENCE

Approved as to style and content by:

Wayne M. Ahr
(Chair of Committee)

Joel S. Watkins
(Member)

Duane A. McVay
(Member)

Andrew Hajash, Jr.
(Head of Department)

May 2002

Major subject: Geology

ABSTRACT

Characterization of the 3-D Properties of the Fine-Grained Turbidite 8 Sand
Reservoir, Green Canyon 18, Gulf of Mexico.

(May 2002)

Matthieu Plantevin, B.Sc. Geology, Ecole Nationale Supérieure de Géologie, France

Chair of Advisory Committee: Dr. Wayne M. Ahr

Understanding the internal organization of the Lower Pleistocene 8 Sand reservoir in the Green Canyon 18 field, Gulf of Mexico, helps to increase knowledge of the geology and the petrophysical properties, and hence contribute to production management in the area. Interpretation of log data from 29 wells, core and production data served to detail as much as possible a geological model destined for a future reservoir simulation.

Core data showed that the main facies resulting from fine-grained turbidity currents is composed of alternating sand and shale layers, whose extension is assumed to be large. They correspond to levee and overbank deposits that are usually associated to channel systems. The high porosity values, coming from unconsolidated sediment, were associated to high horizontal permeability but generally low kv/kh ratio.

The location of channel deposits was not obvious but thickness maps suggested that two main systems, with a northwest-southeast direction, contributed to the 8 Sand formation deposition. These two systems were not active at the same time and one of them was probably eroded by overlying formations. Spatial relationships between them remained unclear. Shingled stacking of the channel deposits resulted from lateral migration of narrow, meandering leveed channels in the mid part of the turbidite system. Then salt tectonics tilted turbidite deposits and led to the actual structure of the reservoir. The sedimentary analysis allowed the discrimination of

three facies A, B and E, with given porosity and permeability values, which corresponded to channel, levee and overbank deposits. They were used to populate the reservoir model. Well correlation helped figure out the extension of these facies.

ACKNOWLEDGEMENTS

I must express my sincere gratitude to Dr. Wayne M. Ahr, chairman of my advisory committee for his guidance and support throughout this research. I would also like to thank to my committee members-Dr Duane McVay and Dr Joel S. Watkins-for their constructive reviews and valuable insight.

I am also indebted to TotalFinaElf for providing the scholarship. Thanks go to many persons at IFP School especially to A. Auriault, G. Gabolde and H. Quicke for their guidance during the Reservoir Geoscience and Engineering program.

I must also thank my parents, my brother and my stepmother for having supported me during the last two years, even if they were far away from me.

Thanks also go to S. Lalande who shared this research with me and helped me on many occasions; all my friends at Texas A&M with whom I shared my happy and sad moments, especially V. Durussel.

TABLE OF CONTENTS

	Page
ABSTRACT.....	iii
ACKNOWLEDGEMENTS.....	v
TABLE OF CONTENTS.....	vi
LIST OF FIGURES.....	viii
LIST OF TABLES.....	x
 CHAPTER	
I INTRODUCTION.....	1
Scope.....	1
Objectives.....	1
Location.....	2
Database.....	2
II BACKGROUND.....	5
Previous work on fine-grained turbidite deposits.....	5
Geological setting.....	10
III METHODS.....	17
Data overview.....	17
Location of the 8 Sand intervals.....	18
Sedimentary analysis of the 8 Sand formation.....	23
Management of porosity values.....	31
Computation of the net thickness.....	31
Choice of facies for reservoir modelling.....	36
IV RESULTS.....	40
Location of the depositional environment.....	40
Map of the top of the 8 Sand reservoir.....	41
Gross thickness map.....	42
Net thickness map.....	42

CHAPTER		Page
	Well correlations.....	45
	3-D reservoir model.....	50
V	DISCUSSION.....	52
	Uncertainties about reservoir shape.....	52
	Continuity inside the reservoir.....	52
	Recommendations for future 8 Sand reservoir simulation.....	53
VI	CONCLUSIONS.....	54
	REFERENCES CITED.....	55
	VITA.....	58

LIST OF FIGURES

FIGURE	Page
1	Location of the Green Canyon 18 field..... 3
2	Oil, gas and water rate from the 8 Sand reservoir from 1987 to 1999..... 4
3	The idealised complete Bouma sequence showing the individual turbidite divisions..... 6
4	Block diagram showing the proposed model for a fine-grained turbidite system..... 8
5	Schematic explanation of the deposition of sheet sands..... 10
6	Structure map of the top salt..... 11
7	Depocenter map of the 1.9-1.4 Ma sequence showing the basin floor fan and the interpreted sediment transport pathways..... 14
8	Depositional model for the northern Gulf of Mexico showing significant sands deposited on downthrown side of major expansion fault..... 16
9	Log response of the 8 Sand interval at well A-2..... 19
10	Log response of the 8 Sand interval at well A-25..... 20
11	Log response of the 8 Sand interval at well A-5..... 20
12	Map showing the trajectory of the wells and the location of the 8 sand intervals crossed by these wells..... 22
13	Core picture showing an angular discordance caused by core twisting in a facies E 24
14	Core picture showing alternating sand and shale layers in a levee deposit..... 25

15	Core picture showing cross ripple lamination in a sand layer.....	27
16	Core picture showing flame structures oriented from left to right.....	28
17	Core picture showing flame structures oriented from right to left.....	28
18	Core picture showing a convolute bedding.....	30
19	Plot showing shaliness values computed from different methods.....	32
20	Comparison between minimum Vsh values from logs and..... Vsh values from cores	32
21	Shaliness-versus-Neutron-Density difference plot.....	33
22	Correspondence between shaliness and Neutron-Density difference.....	35
23	Chart used for facies modelling	36
24	Correlation between porosity values from cores and from logs.....	37
25	Plot showing petrophysical properties of facies A, C and E	38
26	Diagram showing the depositional environment of the 8 Sand reservoir.....	40
27	Map of the top of the 8 Sand reservoir.....	41
28	Gross thickness map.....	42
29	Correlation between half-energy time and reservoir thickness.....	43
30	Net thickness map.....	44
31	Cross-section 1 from well correlation.....	46
32	Cross-section 2 from well correlation.....	47
33	Location of the three cross-sections.....	48
34	Cross-section 3 from well correlation.....	49
35	Reservoir model showing the facies repartition..... within the 8 Sand reservoir	51

LIST OF TABLES

TABLE		Page
1	How to recognize the different facies from their log response.....	21
2	Standard deviation from core measurements for two different shaliness computation methods.....	33
3	8 Sand interval gross thickness, net thickness and net-to-gross ratio.....	34
4	Location of facies with associated porosity and permeability values.....	39

CHAPTER I

INTRODUCTION

Scope

Deep marine turbidite deposits are the focus of major exploration and development efforts in the deep-water area of the Gulf of Mexico and worldwide. In the United States, the Gulf of Mexico is now the primary area of exploration activity for the major oil companies and these reservoirs are capable of world-class flow rates and typically are massive and have large, well-connected areal extents.

This thesis attempts to characterize the main properties of the 8 Sand reservoir in the Green Canyon 18 block, Gulf of Mexico, such as reservoir shape, geological facies repartition and petrophysical properties. Ultimately this study will help perform a reservoir simulation.

Objectives

The overall objective of this study is to increase knowledge of the geology of the 8 Sand turbidite reservoir and to contribute to production strategy from this reservoir. Specifically, this involves an integration of core and well log data to:

- Define and map the shape of the 8 Sand reservoir;
- Populate this body with facies and petrophysical properties;
- Provide some recommendations for a future reservoir simulation;

Location

The Green Canyon Block 18 field is located 70 miles off of the Louisiana coast (figure 1), south of Morgan City (Brinkmann et al., 1985).

Exxon/Mobil is the operator of Green Canyon 18 Field and has a 55% working interest (WI). The other interest owners of the Green Canyon 18 Field are BHP Petroleum (Americas) with a 25% WI, Burlington Resources with a 15% WI, and Kerr-McGee Oil & Gas Corporation with a 5% WI. The development area is a middle slope paleo-environment of Pliocene-Pleistocene age, which is in the “Flexure” trend (Brinkmann et al., 1985). The discovery well, the Green Canyon 18 No.1, was drilled in December 1981 in 760 ft of water and reached a total depth of 13,127 ft MD in April 1982. Additional five exploration/appraisal wells were drilled before the 30-slot platform was set in November 1986. Producing operations commenced in May 1987 (Ostermeier, 1993). Figure 2 shows a production plot for the 8 Sand reservoir, which is the formation that we focused on. The monthly production for the 8 Sand as of October 1999 was 78 MSTB of oil, which correspond to a daily rate of 2,500 STB/D, and 102 MMscf of gas. Cumulative oil production from the 8 Sand reservoir was 7 MMSTB of oil and 8 Bcf of gas in December 1999. From these values, the original oil-in-place was estimated to be between 25 MMSTB and 35 MMSTB of oil.

Data base

Data used for this study included well log measurements from 29 wells throughout the Green Canyon 18 field, as well as core data that was provided by Burlington Resources. Some previous reports about the production area were also obtained courtesy of Burlington Resources. Lee Williams, who worked on the 8 Sand reservoir for his thesis, also provided information about the 8 Sand reservoir.

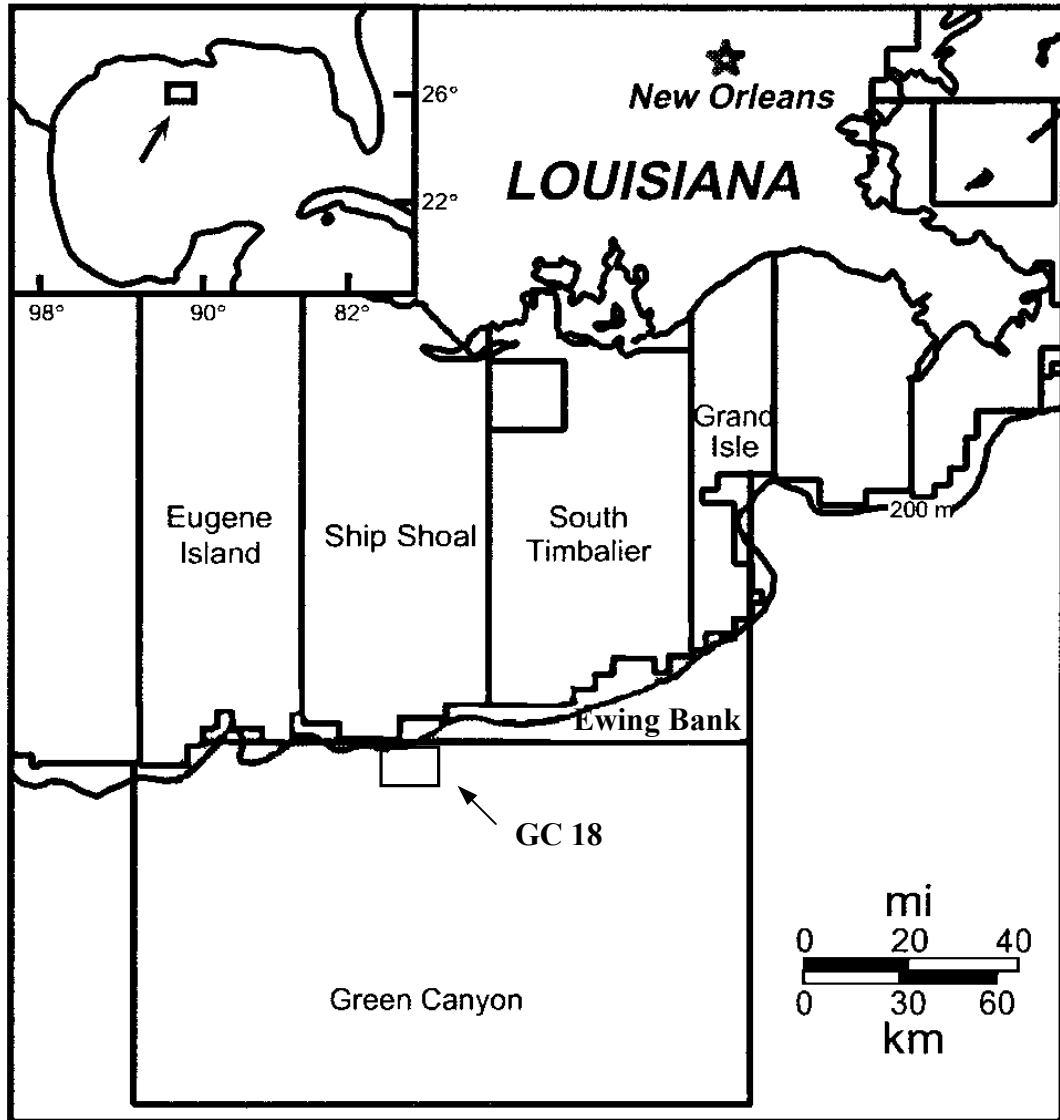


Figure 1-Location of the Green Canyon 18 field (from Weimer et al., 1998).

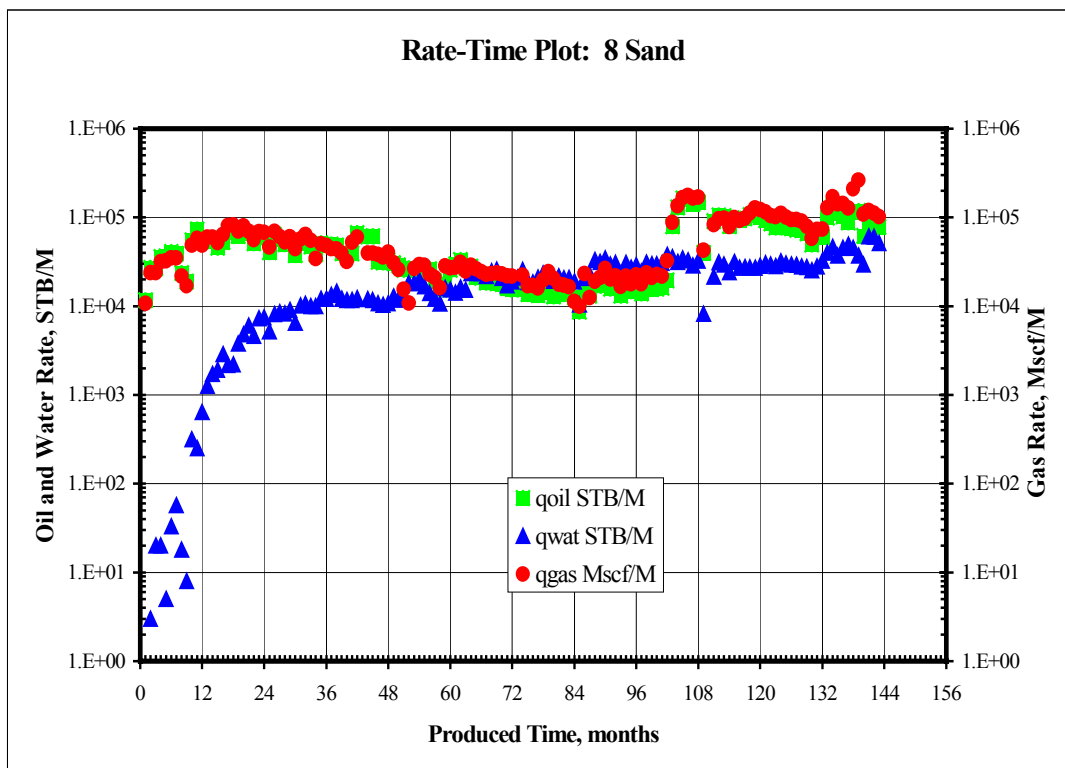


Figure 2-Oil, gas and water rate from the 8 Sand reservoir from 1987 to 1999 (from Williams, 2000).

CHAPTER II

BACKGROUND

Previous work on fine-grained turbidite deposits

Before dealing with the main characteristics of deepwater depositional systems, it is important to focus on the exact terminology of the terms involved in the description of these models. Deepwater depositional systems represent deposition primarily by sediment gravity flows, which transport clastic sediment down a slope and onto a basin floor (Stelting et al., 2000). These systems are called submarine fans when referring to a modern deepwater accumulation exposed on the present-day sea floor (Menard, 1955), or even in some cases to any unconsolidated sedimentary succession. They are called turbidite systems when referring to subsurface and/or outcrop occurrences (Mutti and Normark, 1987, 1991) and commonly to consolidated deposits. Mutti and Normark (1991) define a turbidite (fan) system as “a body of genetically related mass-flow and turbidity-current facies and facies associations that were deposited in virtual stratigraphic continuity”. Bouma et al. (1985a, b, c) called individual unconformity-bounded turbidite systems « fanlobes ». Bouma created a sequence showing the ideal turbidite divisions (figure 3).

When stacked, turbidite (fan) systems and their bounding basinal shales are defined as a turbidite (submarine fan) complex. If the shales or silty mudstones are about the same thickness as the sand-rich beds of the individual turbidite systems or if they comprise at least 70% of the total succession, the system is referred to as being “mud-rich” (Reading and Richards, 1994). According to Stelting et al. (2000), it is recommended to use *turbidite system* (complex) to refer to a composite succession of sand and mud gravity flow deposits that form depositional units of second-, third-, and/or fourth-order depositional sequences as defined by Posamentier et al. (1988). *Deepwater* is also consistent for describing this kind of system.

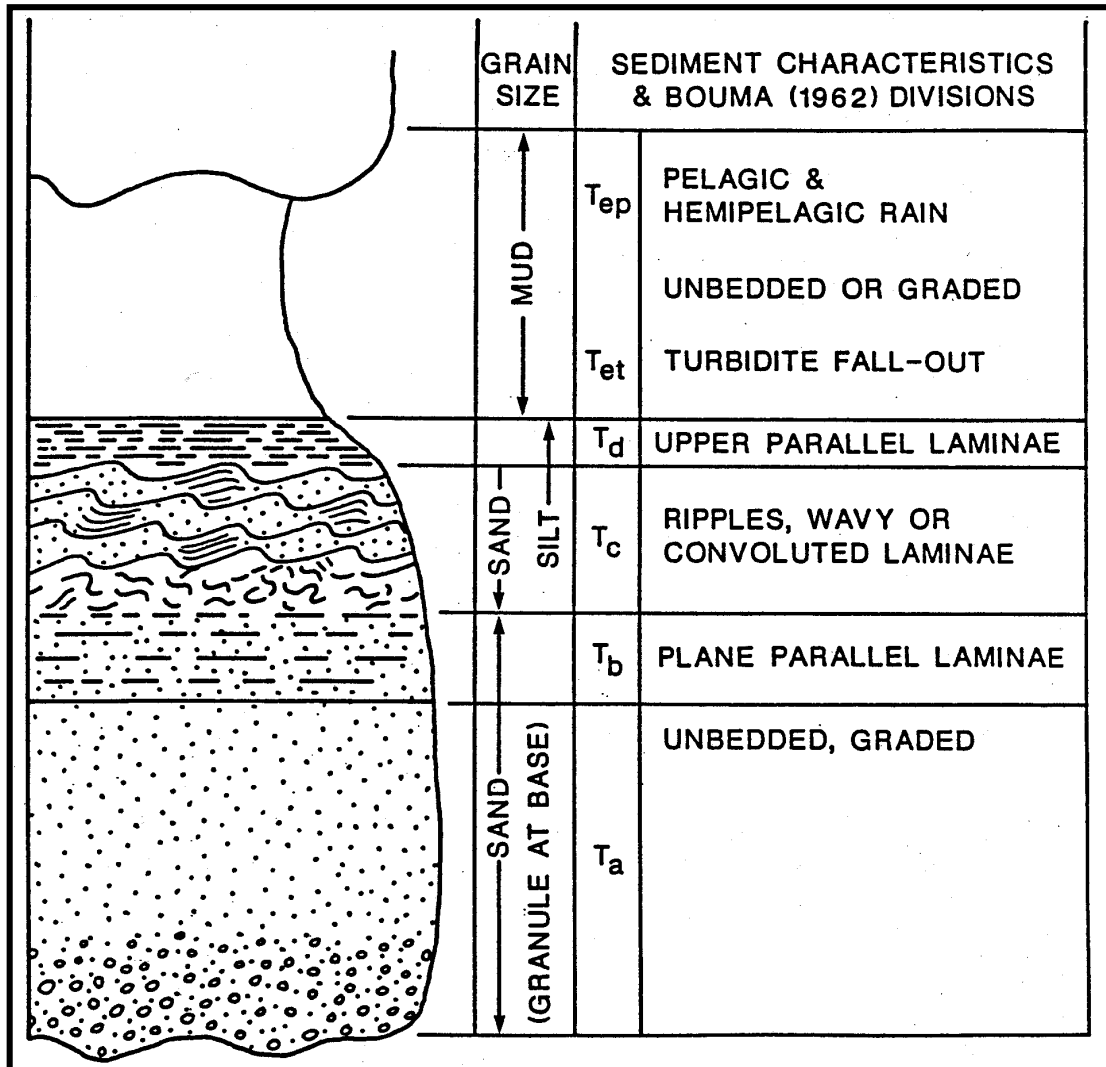


Figure 3-The idealised complete Bouma sequence showing the individual turbidite divisions.

Bouma et al. (1995a, b) proposed to divide a turbidite system into three main parts: inner, mid- and outer zones. Three major parts can be identified with transition zones in between. The base-of-slope, forming the transition from basin slope to basin floor is characterized by a wide channel complex. The mid zone is comprised of a leveed channel with extensive overbank deposits. The lower part of the midfan area contains a transition made up by a distributary channel system. The outer zone is characterized by sheet sands or depositional lobes (Bouma, 2000).

Turbidity flows do not flow continuously, even if fine material is likely to stay in suspension for a few hours. Figure 4 shows that the basin slope is a typical mud province with some local slumps. A major channel feature was formed by the sliding and slumping of large volumes of sediment that accumulated in the upper canyon. This upper fan channel or fan valley serves as the conduit for the transport of sediment toward the basin. It is the last feature to be filled, although some local sandy channel fills and slumps of shelf sands may be present.

The base-of-slope is the zone where the gradient of the slope decreases to that of the upper basin floor. That change in gradient can force several of the gravity flows to start deposition in that zone. The fill of the conduit in the base-of-slope area is comprised of a stack of wide, thin channel fills with some remnants of sand-rich levees and sometimes minor overbank deposits. Locally the channels may erode part of the older ones. Very silty shales may separate the channel sandstones, but the net-to-gross ratio remains high. The channel sandstones are dirty compared with those in the basin because the initial gravity flows had not been able to become well organized.

Since the basin floor is more unrestricted the type of deposition changes into a well-developed channel with levee and overbank sedimentation. Levees focus the direction of the head of a gravity current. The upper part of the main body of the current often spills over the levee, resulting in accumulation on the levee and on the extensive overbank area. The flow that crosses the levee changes from a turbulent flow to a traction current, which leads to the formation of climbing ripples. Traction currents also seem to winnow the sediment, resulting in levee sands that commonly exhibit the highest porosity and permeability values within a turbidite system.

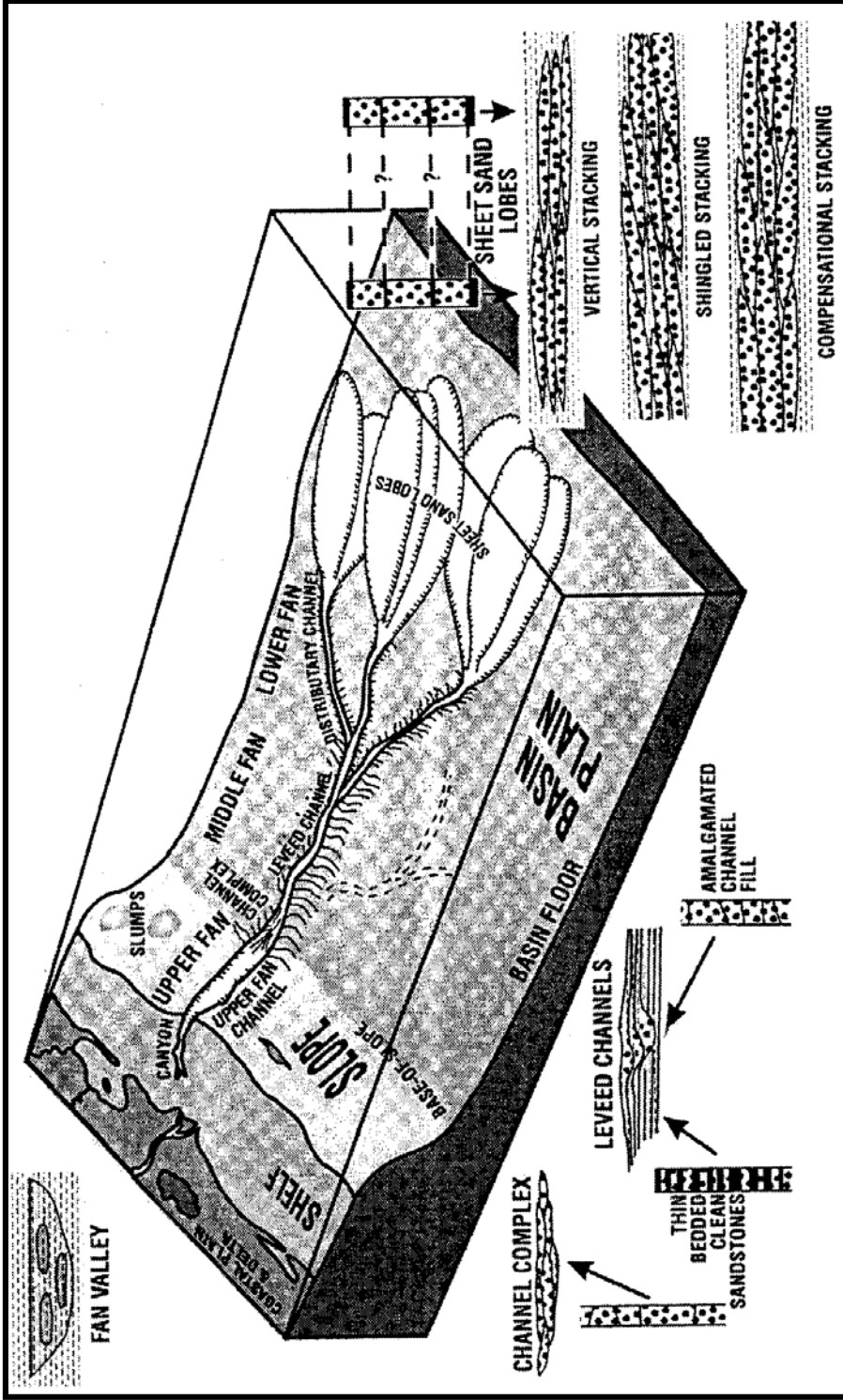


Figure 4-Block diagram showing the proposed model for a fine-grained turbidite system. The three end components of the model (channel complex, leveed channel with overbank areas and sheet sands) are shown in cross section and as an idealized core (from Bouma, 2000).

The channel fill commonly appears to be massive, being comprised of amalgamated sandstones. The levees consist of alternating sandstones and shales. The coarsest and the thickest levee sands can be expected closest to the channel margin, whereas the mud-rich, lenticular-bedded sequences are found in the more distal overbank sites. The sandstones usually contain foreset bedding, climbing ripples, and parallel lamination. The sand-to-shale ratio can vary from 30 to 60%. It can be noticed that the levees of the modern fan channels become progressively smaller (i.e., thinner and less wide) down fan and finally disappear in the lower fan area. The overbank deposits also have sandstone-shale couplets that gradually become finer and thinner away from the channel, with a decreasing of the net-to-gross ratio. The levee deposits are also known as low-resistivity, low-contrast, thin bedded sandstones (Darling and Sneider, 1992). The individual layers are too thin to detect on traditional electrical logs, although they can be excellent reservoirs because of the high porosities and permeabilities (Bouma and Wickens, 1994).

The distributaries become shallower and finally are no longer capable of containing the head of the gravity currents. They overflow the low terminal levees and fan-out, forming an elongate sheet sand, whose shape depends on flow velocity and density, in addition to bottom roughness and shape of the basin floor. Each layer looks more or less plane parallel, except at the sides and distal terminus. Different stacking patterns exist for these deposits. Individual sheets are separated stratigraphically by thin silty layers that are often discontinuous (figure 5).

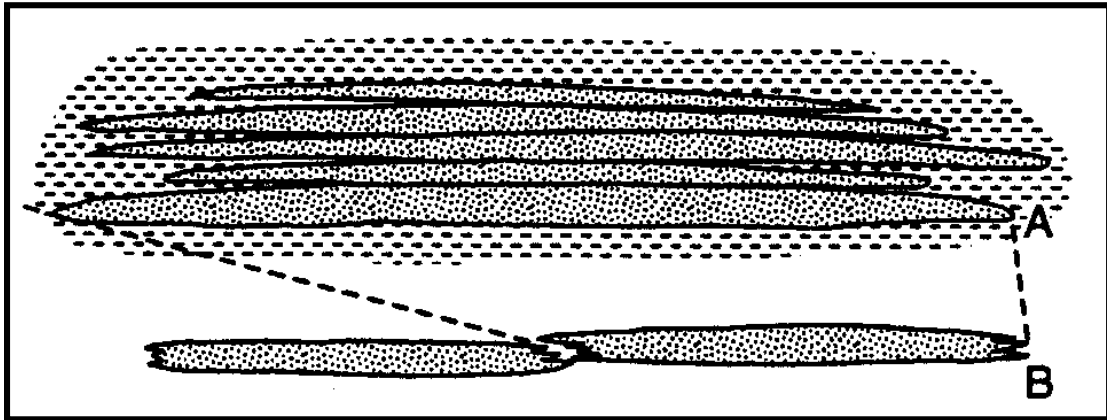


Figure 5-Schematic explanation of the deposition of sheet sands. (A) A succession of individual sandstone layers. Note the amalgamated (or very thin shale) contact between the centers of the slightly convex-shaped sandstones. (B) Two packages of sandstones onlap onto each other. These packages are called sheet sands. Individual sandstones may be 10-80 cm thick; a package can range in width from 500 to more than 1000 m.

Geological setting

A major interest in the Gulf of Mexico is the complex relationship between tectonics and sedimentation in the northern continental slope. A structure contour map of the salt system in Northern Green Canyon/Ewing Bank is shown in figure 6.

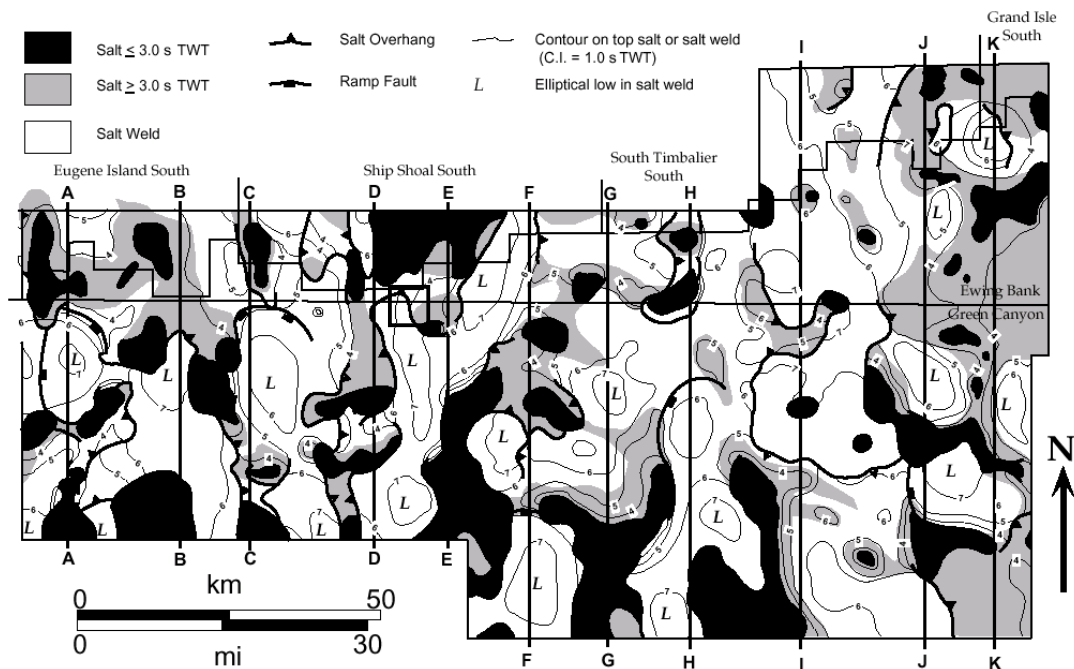


Figure 6-Structure map of the top salt (from Weimer et al., 1998). The black square represents the Green Canyon 18 area.

The most prominent feature of this salt system is its large relief, with the tops of the shallowest diapirs at less than 1.0 s two-way traveltime and the deepest salt welds at more than 7.5 s two-way traveltime. The pattern is a complex one in which different salt bodies have evolved and amalgamated through time to create a composite salt system with multiple levels. Diapirs generally are found along the frontal or lateral edges of shallow sheets. These diapirs usually do not have deep roots and have variable geometries. In plan view, they range from circular to highly irregular. To the north, the salt system is dominated by the southern portions of shallow sheets that extend to the north onto the shelf. These northern areas generally have thin remnant salt between scattered small diapirs with no deep roots, and the diapirs along the southern edges of the sheets commonly have been modified by contractional squeezing. To the south, salt bodies usually are thicker and of larger areal extent, with roots that connect them to the underlying ridges and saddles in the base-salt surface (Weimer et al., 1998).

The different types of salt systems impact the stratigraphic evolution of the minibasins of this area in several ways. First, these salt systems determine the

shifting location and shape of minibasins through time. Second, they define the local sea-floor paleobathymetry during each depositional cycle, and also dictate subsequent basin modification (thereby producing structural traps). Third, the evolution of each type of system determines whether there is adequate underlying salt to provide accommodation for vertical stacking of ponded sands. Thus salt tectonics has a major influence on the geometry of the turbidite reservoirs by impacting the deposition environment of the turbidity currents.

The productive strata in the Green Canyon Block 18 Field occur within a single sequence. The primary reservoirs of Green Canyon 18 are part of a mounded turbidite package that was deposited by density grain flows and debris flows with possible reworking by bottom-hugging, deep water (contourite) currents along the north flank of the Green Canyon salt dome. The main reservoir target sands of Block 18 occur in the bend of the channel complex, on this northern flank. These sands are part of a northwest-southeast trending anticline that is bounded on the south by a southeast dipping extensional fault.

Seismic and geologic facies change abruptly across the area in all sequences, reflecting the lateral and vertical changes in lithofacies from sand-rich to mud-rich systems (Weimer, 1998). The lower reservoirs (e.g., 20, 26 and 30 Sands) are coarser grained and more massive than the shallower reservoirs, which tend to be highly laminated. These sandstones were deposited during the Upper Pliocene and Lower Pleistocene. The Upper Pliocene 8 Sand is in the upper lowstand sequence, within the 1.9-1.4 Ma sequence, also called "CM" sequence. Biostratigraphic data suggest that this sequence is a fourth order sequence. It has been demonstrated that there are spatial and temporal variations of the turbidite deposits throughout the Green Canyon area.

Sheet sands (depositional lobes or basin-floor fans) seem to represent only a minor portion of the sequences in terms of thickness and areal distribution (Weimer et al., 1998). In the 3.0-0.7 Ma sequences, the basin-floor fans do not fill minibasins, unlike the older ones, so their areal extent is less. These kinds of fans were deposited in the downthrown side of growth faults and adjacent to shallow salt bodies in lower bathyal water depths. The tectonic elements helped to create localized bathymetric lows on the sea floor, and the lobes were deposited in these restricted areas. But lobe

fans are not likely to be present during the 1.9-1.4 Ma sequence in the Green Canyon 18 area as we can see in figure 7. The study area was located much closer to the shelf.

One proposed interpretation is that this period was more influenced by faults than by salt tectonics, and that the active large salt withdrawal basins were more effective in trapping coarse-grained sediments than the fault-related basins. Perhaps the abrupt changes in bathymetric relief that caused sand deposition from turbidity currents were greater in these salt-withdrawal basins (Weimer et al., 1998). It could also be related to the increase in clay in turbidity current delivered to the basin.

Concerning the channel-levee systems, it appears that the number and sand content of the channel systems gradually decreased through time throughout the area. Thus channel fills are not common in the 1.9-1.4 Ma sequence, maybe because the large unchannelized flows of mud-rich sediments have become more dominant in the more shaly Pleistocene sequences.

Due to this decrease in channel systems, the overbank deposits, interpreted as mostly shales interbedded with silty sands, are interpreted as large unchannelized flows of mud-rich sediments transported into the area.

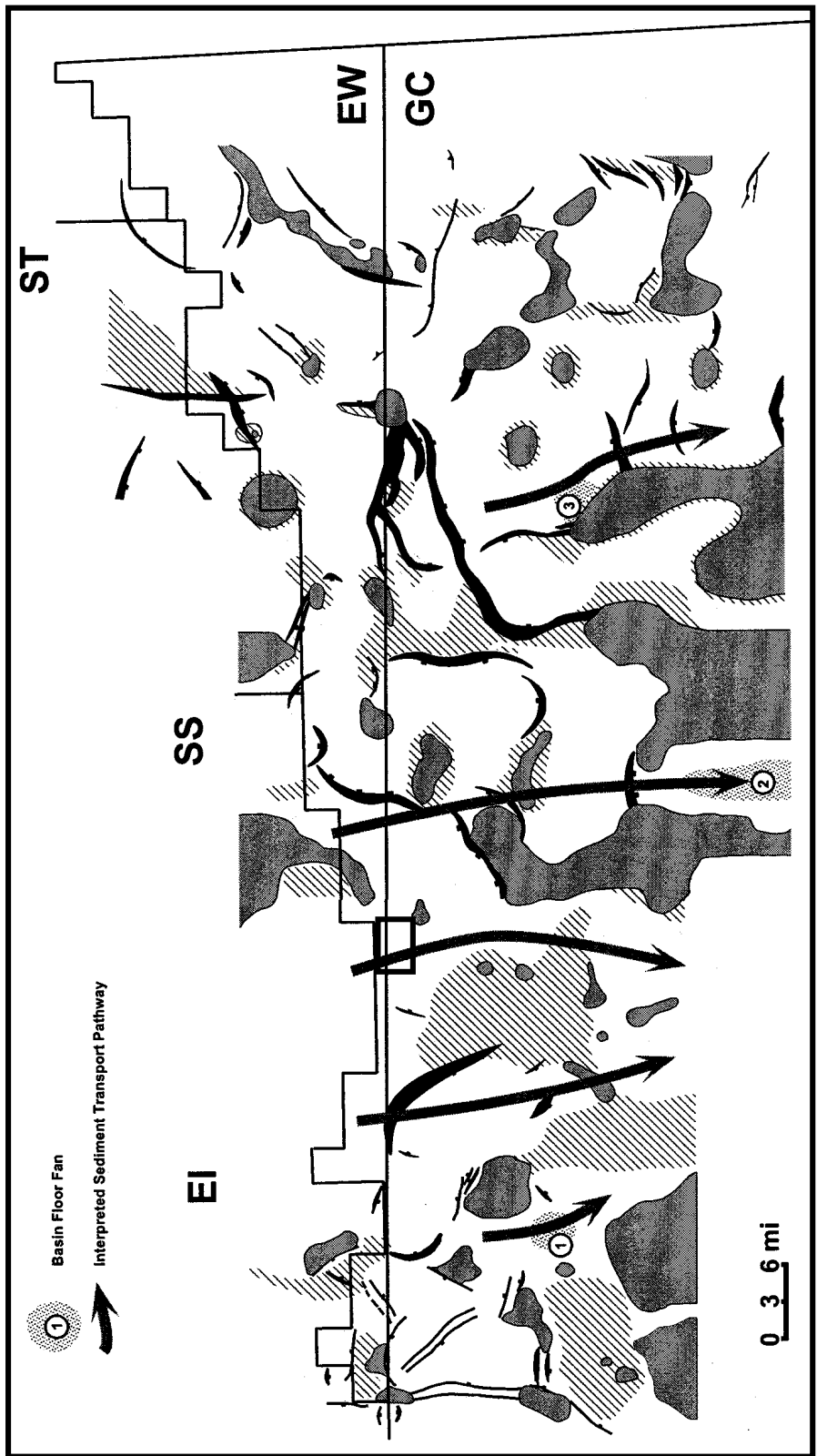


Figure 7-Depocenter map of the 1.9-1.4 Ma sequence showing the basin floor fan and the interpreted sediment transport pathways. The square represents the Green Canyon 18 area (from Weimer et al., 1998).

Turbidity systems are interpreted to be deposited only during major relative lowstands in sea level in the lowstand system tracts. In the transgressive and highstand system tracts, most sediments were trapped in shelf areas; thus hemipelagic shales were deposited in the study area, especially during the 3.0-1.4 Ma interval, where they are interbedded with channels and overbanks.

Another important point is the presence of slides in this area. In the 5.5-1.1 Ma sequences. They are associated with shallow salt bodies and growth faults, and may deform the entire sequences in some minibasins. These slides are interpreted as the result of syndepositional tectonics movements. Some sliding features are present in the 8 Sand succession, as we will see further in this study.

Some previous interpretations showed that sandstones in the upper lowstand system, even if they are highly continuous and exhibit good reservoir properties, extend over much smaller areas than those in the lower lowstand. In addition, the upper lowstand contains a much higher percentage of shale. The sandstones are interpreted as “shingled” turbidites and commonly exhibit excellent porosity and permeability.

A variety of stratigraphic models have been proposed for the distribution of lithofacies in the Gulf of Mexico intraslope turbidite systems. All of these models are viable and reflect the portion of the northern Gulf of Mexico they were drawn from in terms of the style and amount of tectonics and slope gradients. Figure 8 shows one model emphasizing how thick bathyal turbidite systems (lowstand systems tract) preferentially stack on the downthrown side of major normal faults.

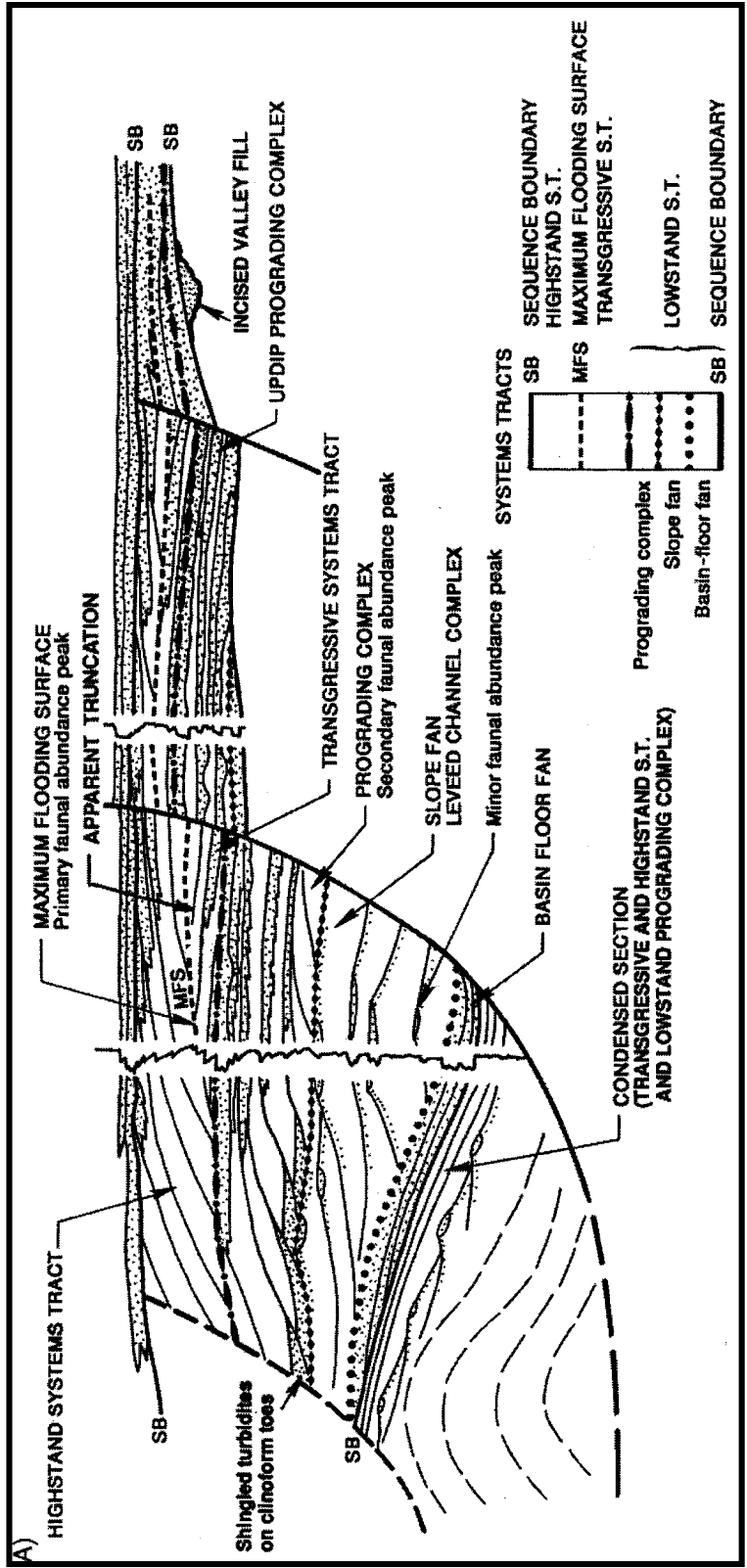


Figure 8-Depositional model for the northern Gulf of Mexico showing significant sands deposited on downthrown side of major expansion fault (from Weimer et al., 1998).

CHAPTER III

METHODS

Data overview

All the data have been provided by Burlington and consist mainly of binders that contain geological, geophysical and production information. Associated to these hard data were furnished digital tapes with 3D seismic and well log data recorded throughout the Green Canyon 18 field.

The well log data concerned more than 30 wells and most of the time comprised all the “classical” measurement such as Gamma-Ray, Caliper, Spontaneous Potential, Spherically Focused laterolog, Medium and Deep Induction Tool, Sonic, Compensated Neutron Log and Formation Density Log. Unfortunately, sometimes only Gamma Ray measurement was provided. A second set of well log data was composed of already interpreted logs such as porosity, shaliness (Vsh) and water saturation logs.

Associated to these log data were provided core measurements that had been performed in several wells in the Green Canyon 18 field. These core analysis were performed by Petroleum Testing Service, Inc., Houston, Texas, and gave information about porosity, permeability, oil and water saturation, apparent sand grain density and lithology of the 8 Sand reservoir.

There were some limitations in the using of these data. First it was soon clear that only a little part of the cores were taken in the 8 Sand interval. Secondly the porosity core values were not likely to represent those within the reservoir, since the pressure conditions were obviously not the same. It was difficult to determine the order of magnitude of discrepancies between these values because different mechanisms are involved, such as rock and fluid compressibility, or fluid pressure that counterbalance the lithostatic pressure inside the reservoir. Nevertheless, some authors assumed that conventional and sidewall core data read lower than in-situ

porosity because of what they call the “snowball effect” (Dunham, 1995). Thus these values have to be carefully examined before being used. Another limitation concerned the fluid saturation of the rock samples. Since the total fluid saturation never reached 100% in all the cores, only the oil/water ratio was likely to give relevant information about the volumes of hydrocarbons present in the reservoir. Thus we extracted saturation values from previous studies on 8 Sand reservoir.

Location of the 8 Sand intervals

The first step of the study consisted in locating the 8 Sand intervals in the wells. Former studies had been already performed, showing the depth of the 8 Sand intervals in 16 wells. We checked if these figures were adequate and tried to look for other wells crossing the 8 Sand formation. The main difficulty consisted in the log response of the 8 Sand that is not homogeneous throughout the field. In some wells the log response was very close to the shale response. Figures 9, 10 and 11 show three examples of 8 Sand log responses.

In well A-2, a 9-feet thick interval between 10900 and 10909 ft MD was assumed to be a channel fill deposit. Indeed the Gamma Ray value is quite low compare to the surrounding facies, the resistivity values are high and the Neutron-Density difference revealed a massive sand signature. Below there is also a 2-feet thick sandy interval that could represent the lateral extremity of another channel. We also noticed that a 4-feet thick shale layer, which could give some information about connectivity between stacked channels, separated these two sandy levels. The rest of the interval is composed of levee and overbank deposits, with high Gamma Ray, low resistivity and Neutron-Density difference close to the one of shale (Low-Resistivity Sand response). No core data were available for this well.

In well A-25, the base of the reservoir between 9960 and 9990 ft MD is very sandy, even if the rapid variations of the shallow resistivity tool are in favor of laminated facies. Two small intervals seem to be channel deposits, for the same reasons as in the previous well. The very high permeability vales in this zone tend to

confirm this assumption. This is one of the best log responses among all the wells crossing the 8 Sand reservoir.

In contrast, A-11 log shows a shalier part of the 8 Sand reservoir, with lower resistivities. This finer material was certainly deposited further from the channel body, forming what we call overbank deposits. This well was located eastward from A-25. This is the typical response of a low-resistivity sand. The resolution of the tools is too low to take into account all the thin layers of sand and shale. The tools integrate the data on an interval in such a way that the response of the shale layers overcomes the one of the sand layers.

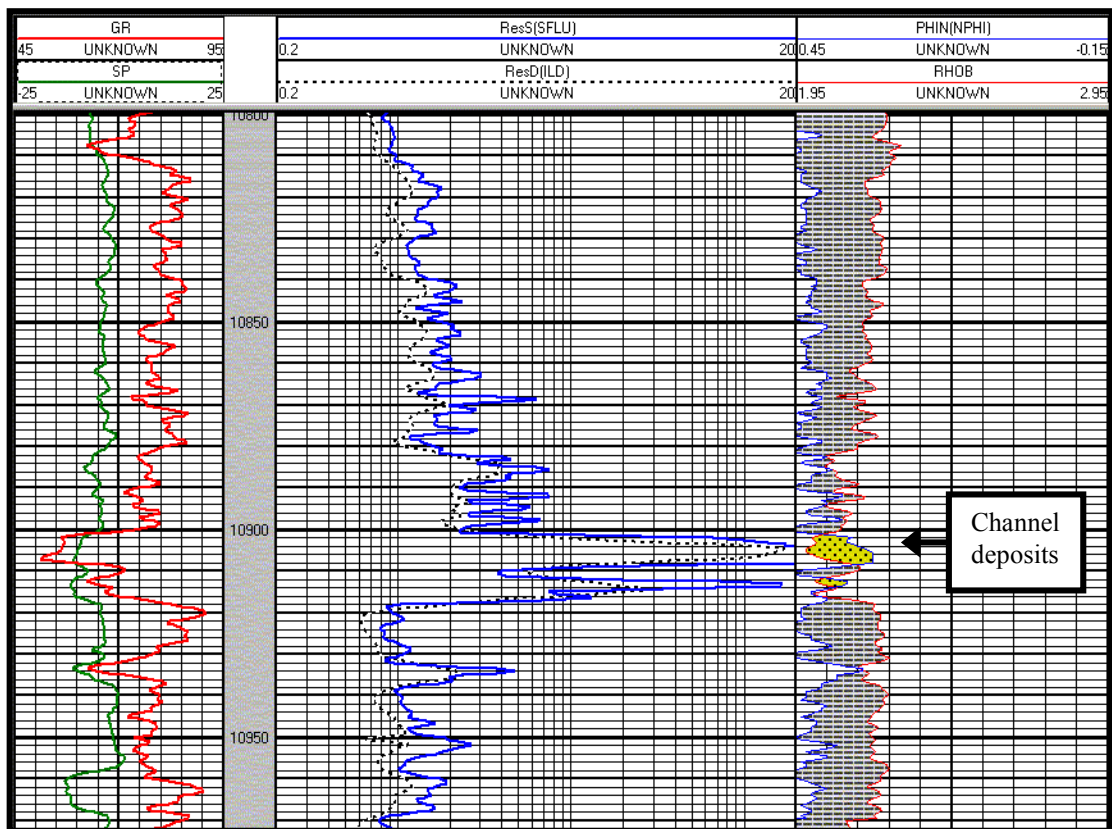


Figure 9- Log response of the 8 Sand interval at well A-2. The depths are in ft MD. Note the channel fill interval between 10900 and 10909 ft.

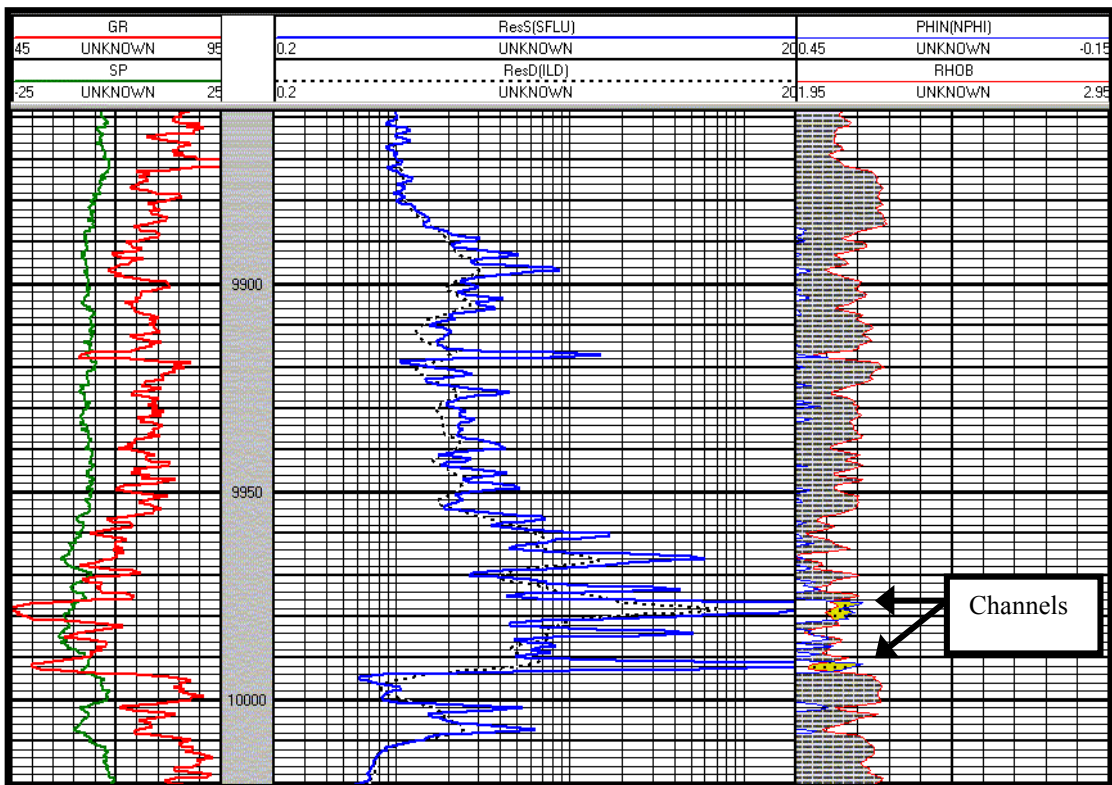


Figure 10-Log response of the 8 Sand interval at well A-25. The depths are in ft MD.

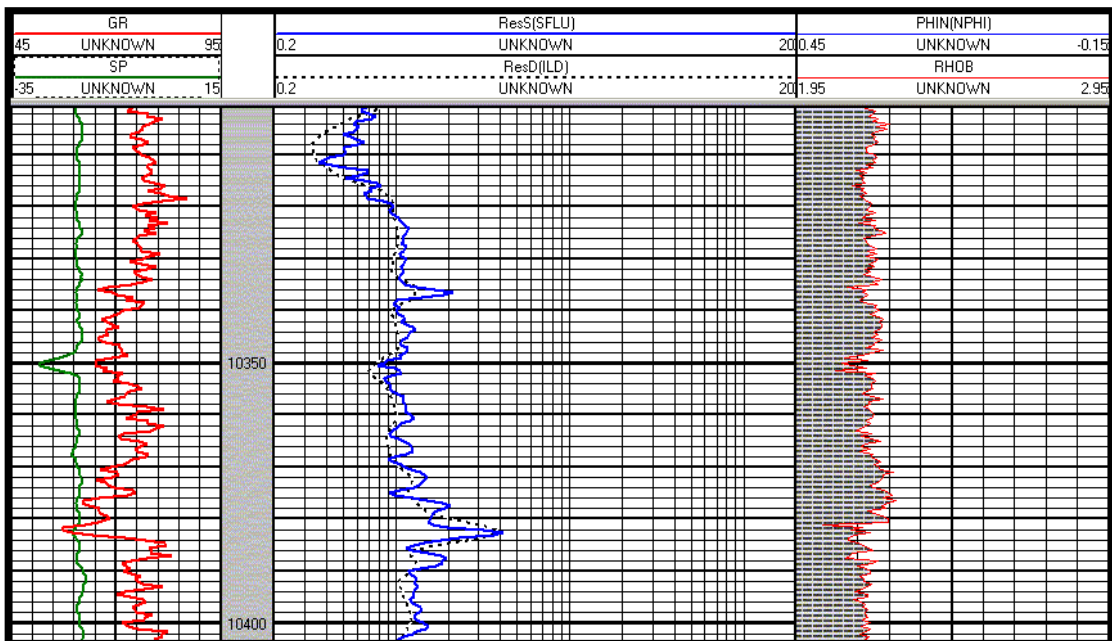


Figure 11-Log response of the 8 Sand interval at well A-5. The depths are in ft MD.

Thus the main characteristics of the 8 Sand reservoir response are:

- Slight decrease of the GR values,
- Slight decrease of the borehole diameter indicating the presence of mud-cake,
- Increase of the resistivity, with a difference between the shallow and the deep measurements,
- Deviations of the sonic towards lower velocities, which may indicate unconsolidated rocks in the 8 Sand formation.

Table 1 sums up the log response of the channel, levee and overbank deposits.

Table 1. How to recognize the different facies from their log response.

	Gamma-Ray log	Resistivity log	Density-Neutron log
Channel	Low, less than 60 API	More than 20 Ω .m	Inversion of the Neutron and Density curves (decrease of the Neutron porosity value)
Levee	Around 75 API	Between 2 and 10 Ω .m	Close to the shale response, Neutron and Density curves are closer from each other
Overbank	More than 80 API, very close to shale response	Less than 2 Ω .m	Neutron-Density difference higher than for levee deposits

Most of the 8 Sand intervals have a “low resistivity sands” response that made their geological and petrophysical characterization quite difficult to establish. Some errors to be avoided had already been highlighted by companies for Green Canyon 18 log interpretation:

- Gamma Ray can not be used to compute bulk volume shale,
- Resistivity will read incorrectly 95%-99% of the time in zones of interest.

Even if some wells seemed to cross cleaner layers, the thickness of these intervals (usually below the tool resolution) indicated that no well crossed a channel fill deposit in the whole field except well A-2, which presented a good log response. This lack of information prevented us from locating with accuracy the channel fills inside the 8 Sand reservoir, even if the impact of such a body in reservoir simulation may be dramatically high. These uncertainties about the channel location should be taken into account in the future 8 Sand reservoir simulation. The location of the wells, their trajectory and the location of the 8 Sand interval are displayed in figure 12. We can see on this map that some wells are highly deviated.

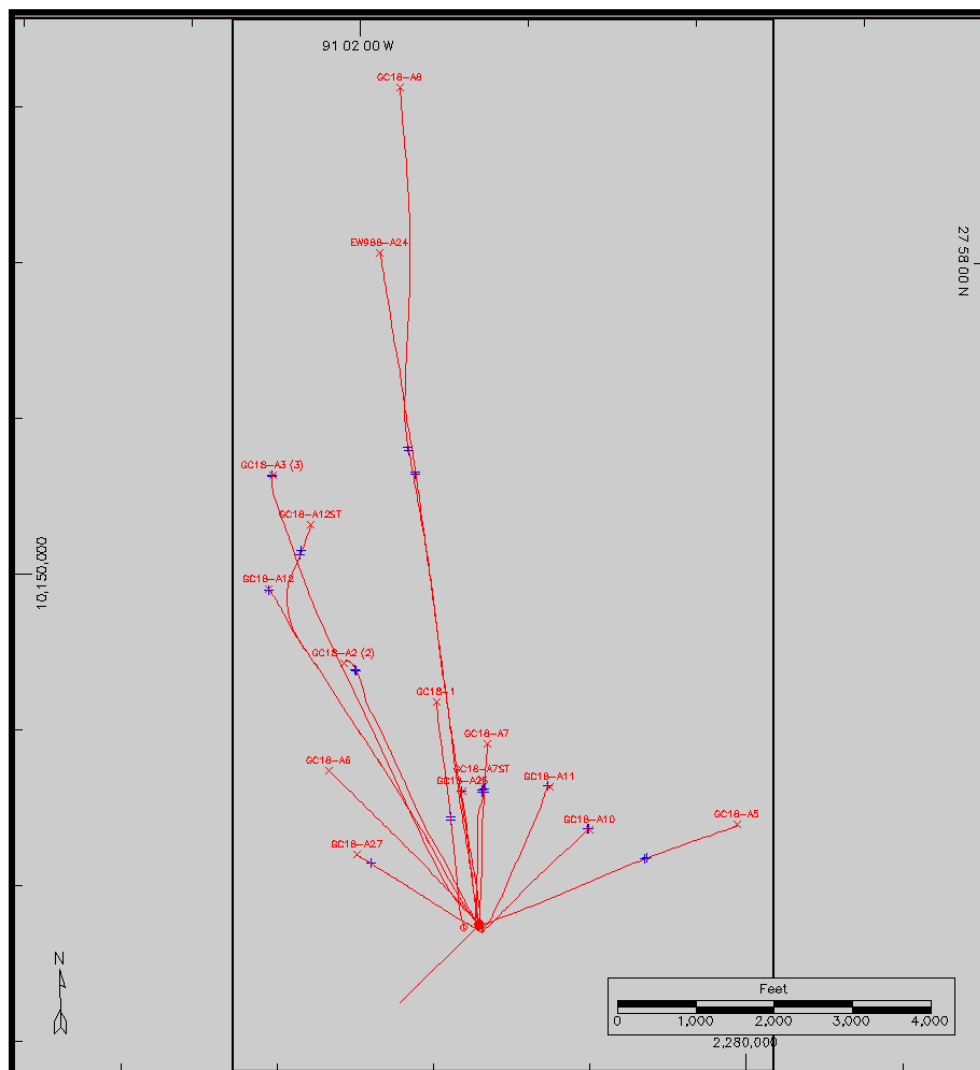


Figure 12-Map showing the trajectory of the wells and the location of the 8 Sand intervals crossed by these wells.

Sedimentary analysis of the 8 Sand formation

This sedimentary study was only based on one set of core pictures from well A-7. These pictures represent conventional-well cores (4 inches) coming from the Green Canyon 18 area. They were examined in order to describe some sedimentary features, determine the principal sedimentary facies, determine environments of deposition and, if possible, relate sedimentary facies to reservoir quality. The described interval was comprised between 9961 ft and 10050 ft. Since most of the wells are deviated in this field, the depths noted are the measured depths, and not corrected “true vertical depths”. Coring was not continuous through this interval. Core recovery was reported to be good, but because the sediment was almost totally unlithified, dislocation and twisting of core was common (McPherson, 1987). This may be a problem for pressure drop during production. The core twisting appeared to be responsible for most of the angular discordance of bedding observed in the core, as we can see in figure 13.

But some of these angular discordances had probably resulted from levee slumping, since the interbedded sand/mud character of the levee deposits form competent and incompetent layering, which is conducive to failure on the relatively high gradients of the levees.

Since we had no actual cores or other rock samples, it was impossible to examine in detail the texture of the layers or the grain size. Looking at the whole interval led to the main conclusion that the facies are quite similar, with some trends that show some evolution of the depositional environment with time. The most common facies is a thinly interbedded deposit consisting of thin beds of well-sorted, very fine-grained sandstone and mudstone. The contacts between sand and shale layers are usually sharp, without any erosion features. We can see these alternating thin layers in figure 14.

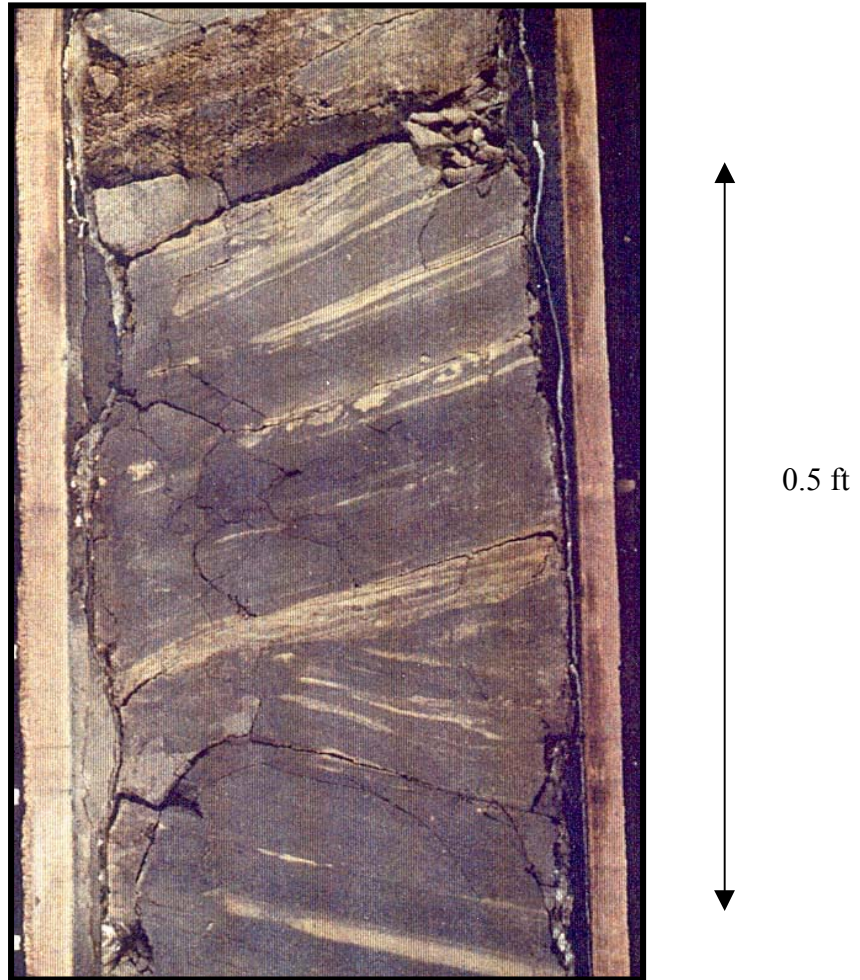


Figure 13-Core picture showing an angular discordance caused by core twisting in a facies E. This core comes from well A-7, at a depth of 9994 ft MD.

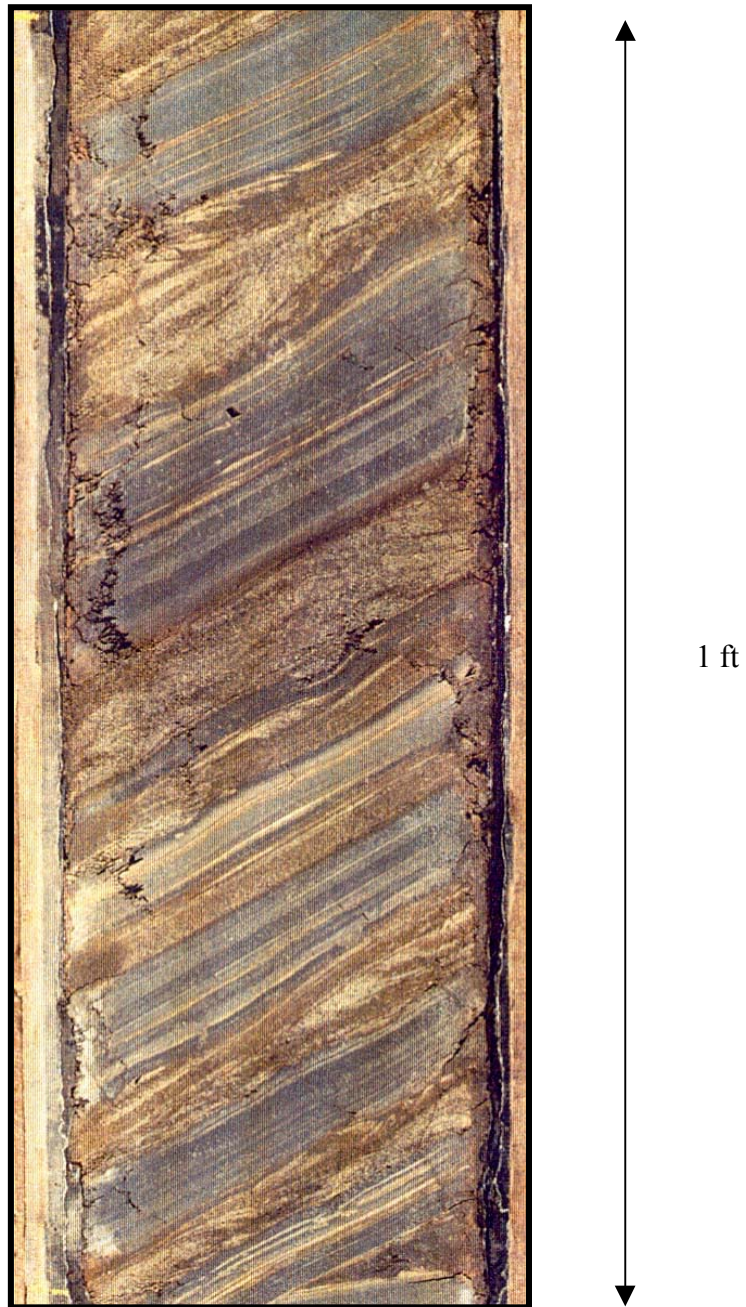


Figure 14-Core picture showing alternating sand and shale layers in a levee deposit (facies C). This core is taken from well A-7, at a depth of 10034 ft MD.

This facies displays various types of lenticular, wavy, and flaser bedding. Distinction between these types is based on the sandstone-to-mudstone ratio (Reineck and Singh, 1973). The individual sand layers show a thickness range of 0.1-3 inches, although locally sand beds up to one foot thick are present. We interpreted these thickness variations as an indicator of the position of the deposit with respect to the channel location. The sand content was computed by measuring the thickness of the sandstone and mudstone layers, and was mostly in the range of 30-70%. In some cores we could detect some fining-upward trends.

The sands are either parallel laminated, or display asymmetrical ripple cross-lamination (figure 15). Climbing ripples, indicative of rapid aggradation, are present in some units and are an indication of a traction current that was present in the edges of the channel.

Some flame structures could be distinguished in the cores, giving an idea of the direction of the main current during the deposition. Their orientation was consistent with the flow direction indicated by the ripples in the same core. Figures 16 and 17 show flame structures present in the 8 Sand interval.

It was interesting to note that the direction of these flame structures is not constant through the whole interval, which can be related to changes in the spatial organization of the turbidite system. Some authors think that this turbidite system was composed of narrow (several hundred feet wide) meandering channels that were migrating laterally with time. This could explain the features described above. Nevertheless the degree of sinuosity of the channels is unknown. Studies on modern submarine fans also suggest that only one channel was active at any one time. Channel shifting, either by gradual sideways migration (lateral migration), or by sudden breakout and establishment of a new channel (avulsion) was a major factor in controlling channel-sand geometry in deep-sea fan systems such as the one in Green Canyon 18 field (Damuth et al., 1988).



Figure 15-Core picture showing cross ripple lamination in a sand layer. The relatively coarser sand is indicative of a deposit close to a turbidite channel. This core was taken from well A-7, at a depth of 10036 ft MD.

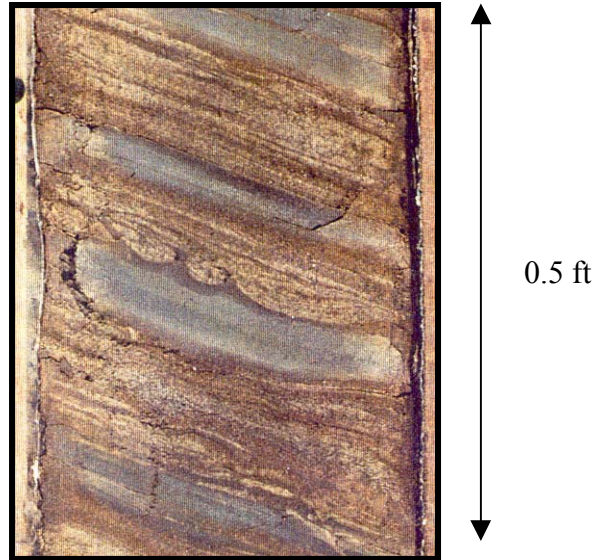


Figure 16-Core picture showing flame structures oriented from left to right. This core was taken from well A-7, at a depth of 10027 ft MD.

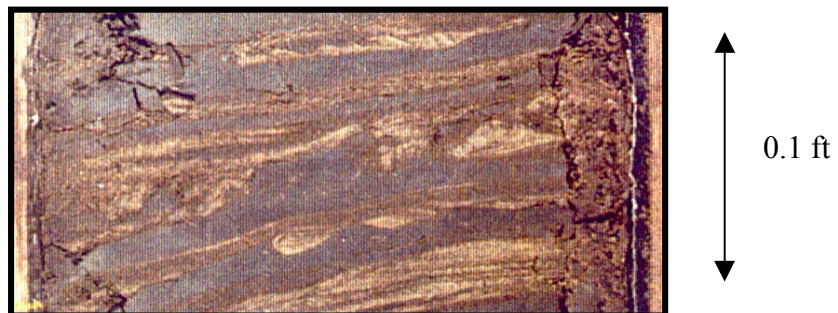


Figure 17-Core picture showing flame structures oriented from right to left. This core was taken from well A-7, at a depth of 10011 ft MD.

Convolute bedding and small-scale loading structures were also present in some cores (figure 18). These structures point to conditions of rapid deposition (Brenchley and Newall, 1977). Some portions of the cores contained more mudstone facies, indicating a deposition further from the channel.

All these remarks were consistent with a turbidite interpretation. These bedded facies could be interpreted to be deposits of relatively fine-grained sediment from both traction and suspension modes.

Because the thickness of the larger sand layer did not exceed 2 feet, we concluded that no channel-fill deposits were visible on these core pictures, even if at some locations of the interval the deposits are likely to be adjacent to a channel. We also inferred that the vertical permeability inside the reservoir should be very low, regarding the laminated nature of the deposits. Thus the k_v/k_h ratio used in the reservoir simulation should be very low. It is important to note that sedimentary features such as ripples or convolutes are likely to interfere with fluid circulation because they create a preferential path for the fluids in motion. Sometimes the contact between channel and levee facies is interpreted as a barrier to fluid flow because there may be a shale interface between the two facies. We did not have any information about the lateral extent of the shale layers, but it is usually admitted that levee and overbank deposits are likely to present good lateral continuity.

Reservoir quality in the Green Canyon 18 field seems to be controlled mainly by permeability. In general, reservoir quality in the sands is high, with porosities around 35% and permeabilities, which can reach 3300 mD. One of the main features in Green canyon 18 cores is that the sediments are unconsolidated because diagenetic modification of depositional porosity and permeability is minimal (Beard and Weyl, 1973). Thus reservoir quality is principally controlled by depositional facies.

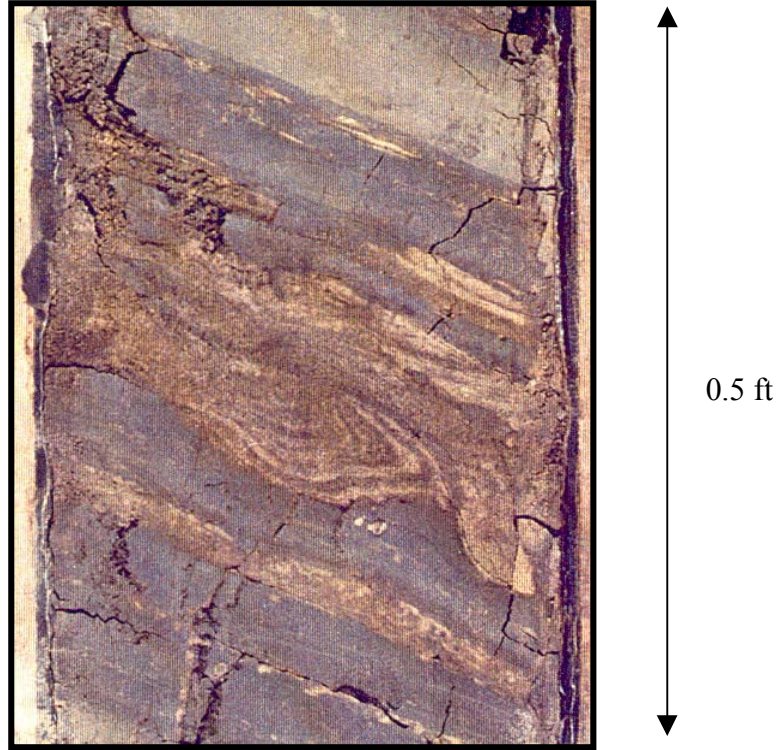


Figure 18-Core picture showing convolute bedding. This core was taken from well A-7, at a depth of 9966 ft MD.

Management of porosity values

8 Sand porosity values derived from cores were only available on six wells in the Green Canyon 18 field. These wells were A-25, A-12, A-7, A-8, A-11 and A-27. Most of the data concerned wells A-7 and A-12.

All the porosity values are high in the 8 Sand reservoir. In this kind of deposits, the high porosities at these depths are attributed to combined effects of excellent grain sorting, high pore pressure, and minimal cementation (Reedy and Pepper, 1996).

Computation of the net thickness

One of the main objectives of this study was to determine the net thickness of the 8 Sand formation. The main parameter that we had to deal with was the shaliness (Vsh). Shaliness is usually computed from log data thanks to different tools: Gamma Ray, spontaneous potential and Neutron-Density. We could not use the Gamma Ray method because of the high-Gamma Ray response of the 8 Sand: we would have overestimated the shaliness value. Thus we tried to compute it with the two other methods.

In parallel we decided to use the core pictures in the purpose of measuring the amount of shale and sand in the cores. In this objective, we measured the thickness of the sand and shale layers, and converted these values into percentages. Even though the precision of measurements was not absolute we could obtain a good approximation of the reality. Then we tried to fit these values with the ones calculated from logs. Unfortunately, due to the bad resolution of the tools, the results were not really consistent. Some shaliness values from previous studies, based on core measurement, were also available, and were used as reference values. Many discrepancies exist between the log values and the measured values, as illustrated in figures 19 and 20. We could not find the evidence of a correlation between the different wells. Table 2 shows the standard deviation between the core values and the computed values from the Gamma Ray and the Spontaneous Potential tools.

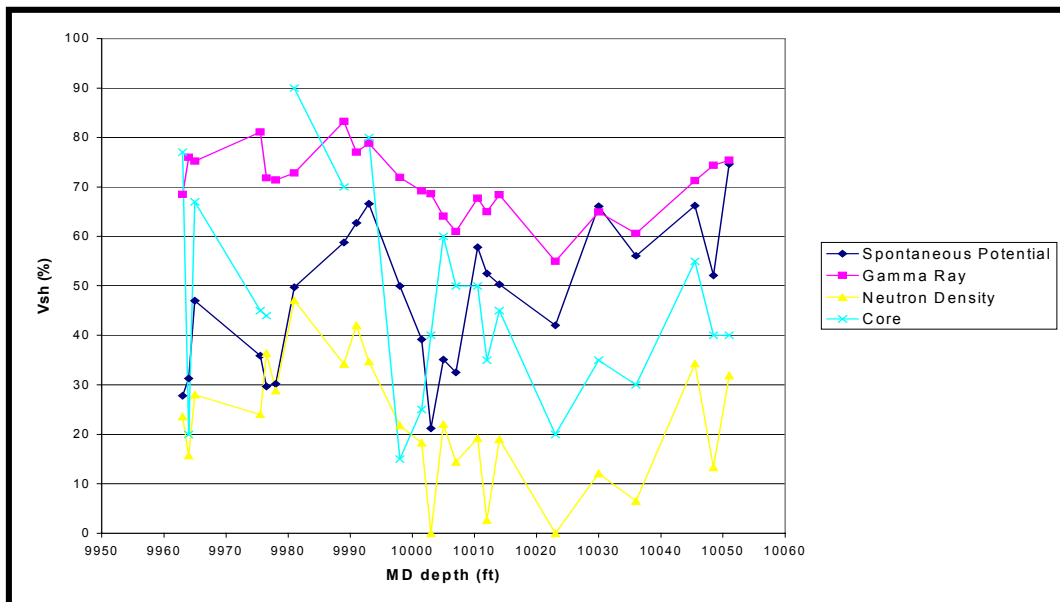


Figure 19-Plot showing shaliness values computed from different methods.

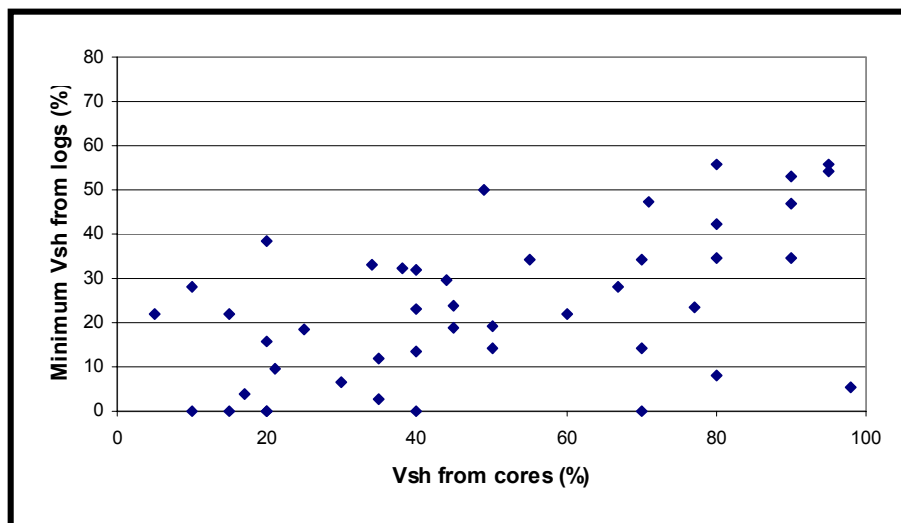


Figure 20-Comparison between minimum Vsh values from logs and Vsh values from cores.

Table 2. Standard deviation from core measurements for two different shaliness computation methods.

Methods	A-7	A-8	A-25
Gamma Ray	35.66	34.95	19.3
Spontaneous Potential	26.39	17.95	32.13

We can see that it is impossible to distinguish which tool response is the most appropriate for the shaliness computation. And it was clear that the Vsh values would not be representative of the sedimentary nature of the 8 Sand reservoir.

Thus we decided to use the measurements from the core pictures from well A-7. Once shaliness values were available for the whole interval, we tried to associate a given range of shaliness values to a given difference between the Neutron and the Density curves, because this value appeared to be quite correlated to shaliness (Figure 21).

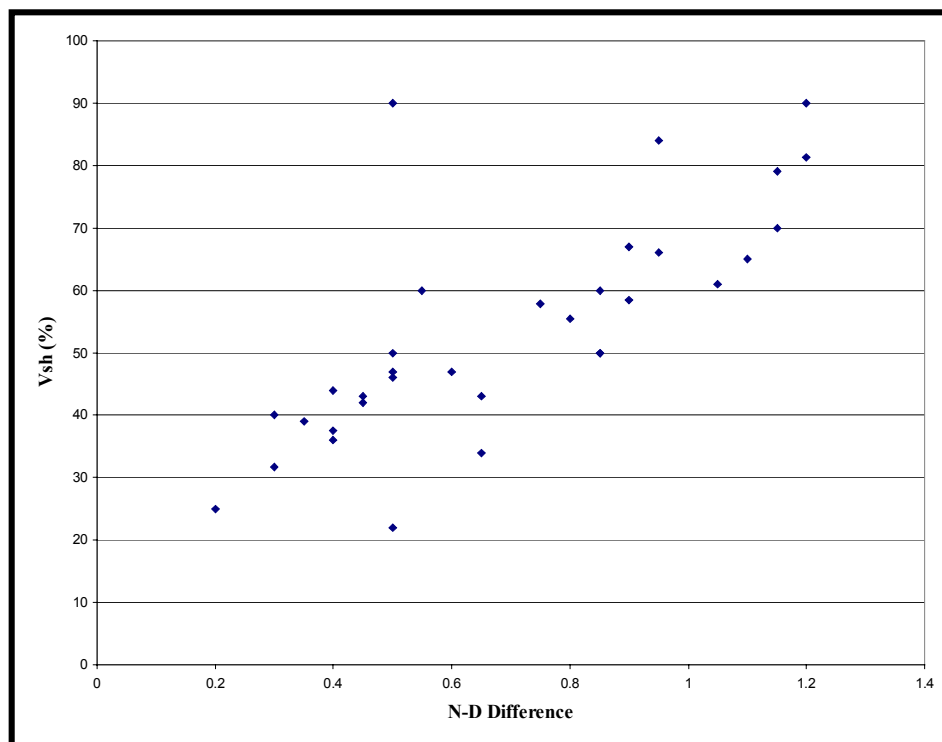


Figure 21-Shaliness-versus-Neutron-Density difference plot.

Finally we obtained a correspondence between shaliness and these curves that is visible in figure 22.

Then we used the Neutron and Density curves in the other wells in order to find shaliness in the 8 Sand interval. Since we associated a given shaliness value to a given thickness in each of the wells, we could compute the net thickness by using the following relationship:

$$h_n = \sum_i Vsh_i * h_i$$

Where h_n is the net thickness and Vsh_i is the average shaliness of an interval of gross thickness h_i . The sum of the h_i is equal to the gross thickness of the 8 Sand interval in a given well. We assumed that the relationship between shaliness and log response in well A-7 was applicable for all the wells. Finally we obtained net thickness values (table 3).

Table 3. 8 Sand interval gross thickness, net thickness and net-to-gross ratio.

Well	Gross thickness (ft)	Net thickness (ft)	Net-to-gross (%)
1	72	35	48.6
A-2	154	76.5	49.7
A-3	146	72.5	49.7
A-5	35	14.8	42.3
A-7	126	58.7	46.6
A-7st	126	54.3	43.1
A-8	53	26	49.1
A-11	71	30	42.2
A-12	89	35	40
A-12st	130	52	40
A-25	121	59	48.8

It is obvious that the reservoir thickness is quite heterogeneous throughout the Green Canyon 18 field. It was interesting to note that the thinnest part of the 8 Sand Reservoir is located in the northern part of the area. One possible explanation is that the northern zone was by-passed by the flow of sediments transported by the

turbidity current. We can see that the average net-to-gross ratio is close to 0.5, which is consistent with the laminated nature of the 8 Sand formation.

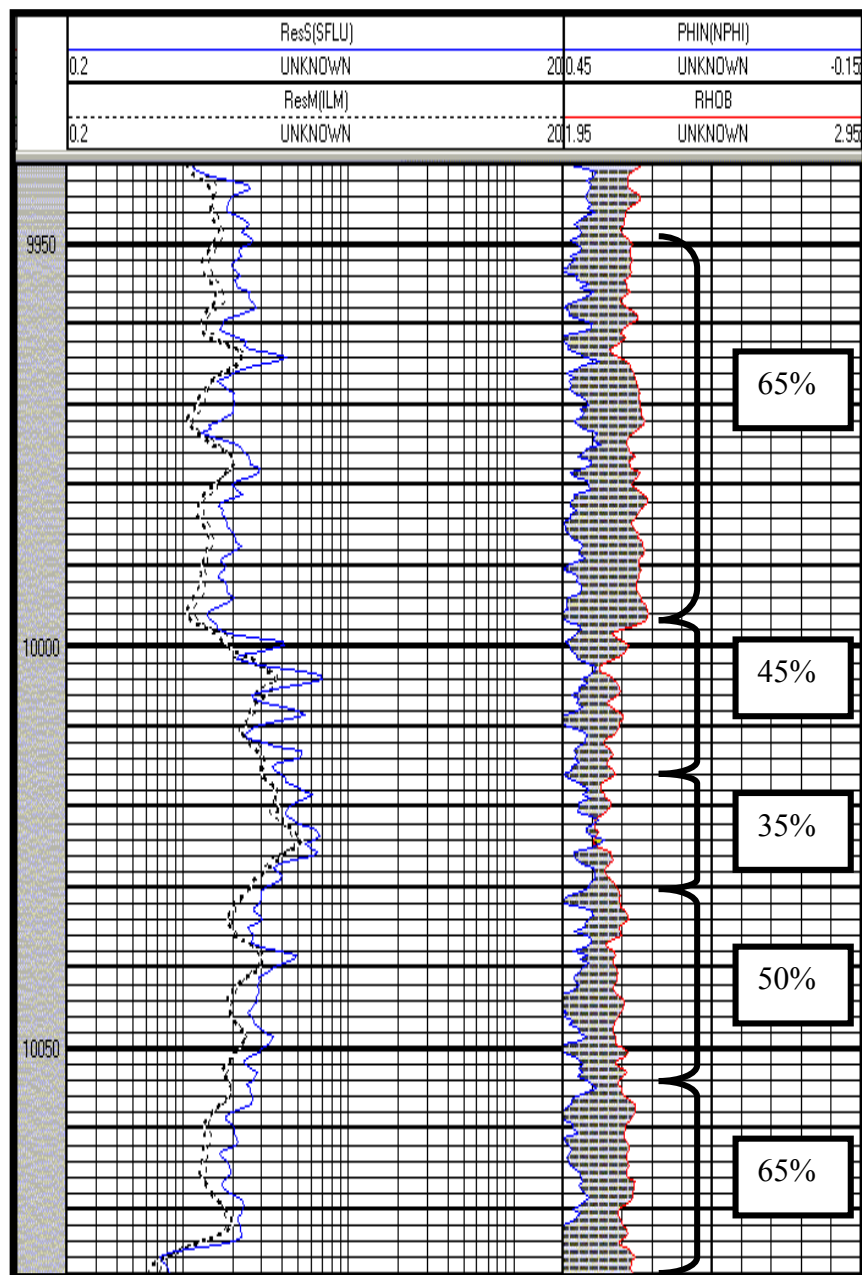


Figure 22-Correspondence between shaliness and Neutron-Density difference. These curve data were from well A-7. Depth values are in feet MD.

Choice of facies for reservoir modeling

Core Analysis Incorporated provided some core data such as permeability, porosity or fluid saturation. It also proposed a sidewall core lamination chart in which sedimentary deposits were sorted into several facies. Taking into account the results previously obtained in our study we decided to sort the sedimentary facies encountered in the 8 Sand reservoir into three main classes that are described in figure 23.

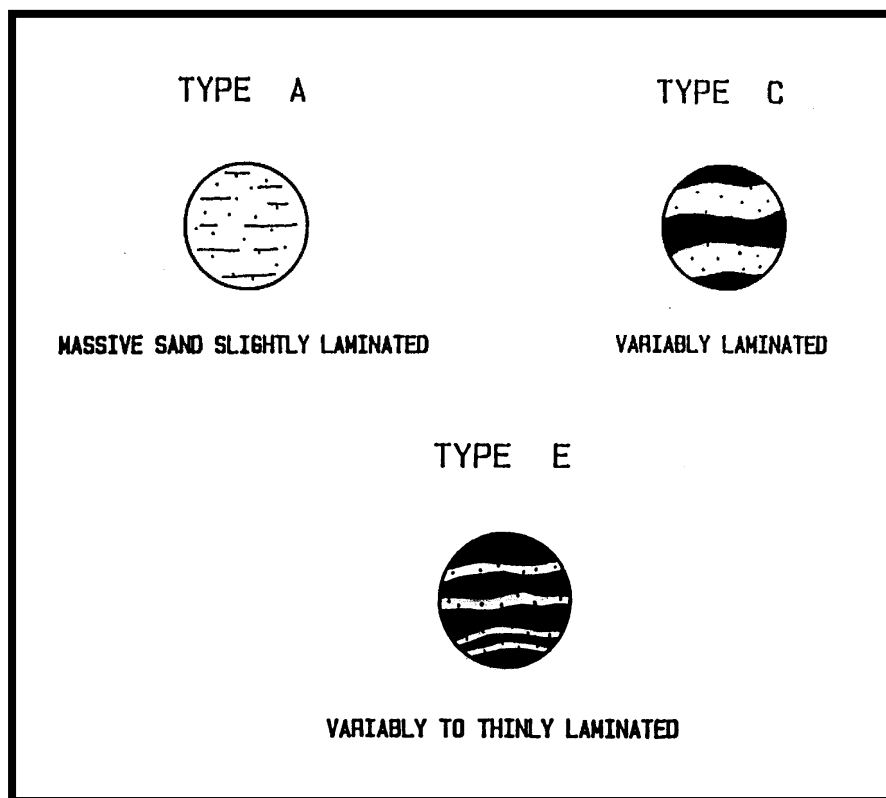


Figure 23-Chart used for facies modeling.

Facies A is mainly associated to channel deposits while facies C and E are linked to levee and overbank deposits respectively. The main idea was to associate these facies with petrophysical properties such as porosity and permeability in order to run a reservoir simulation later on. These facies were recognized in two wells of Green Canyon 18 field: A-8 and A-11. Thanks to core pictures of well A-7 we

managed to describe these facies in this well. Then we tried to locate these facies in all the wells thanks to the criteria described in the previous sections. Once all the well intervals were populated with facies, we decided to associate each interval with porosity and permeability values.

The first step consisted in computing the porosity values in the wells where no core data were available. Based on previous studies concluding that porosity values derived from density values were the most accurate ones (Dunham, 1993), we used the density tool to obtain porosity. Figure 24 shows the quite good correlation between porosity values from density log and core.

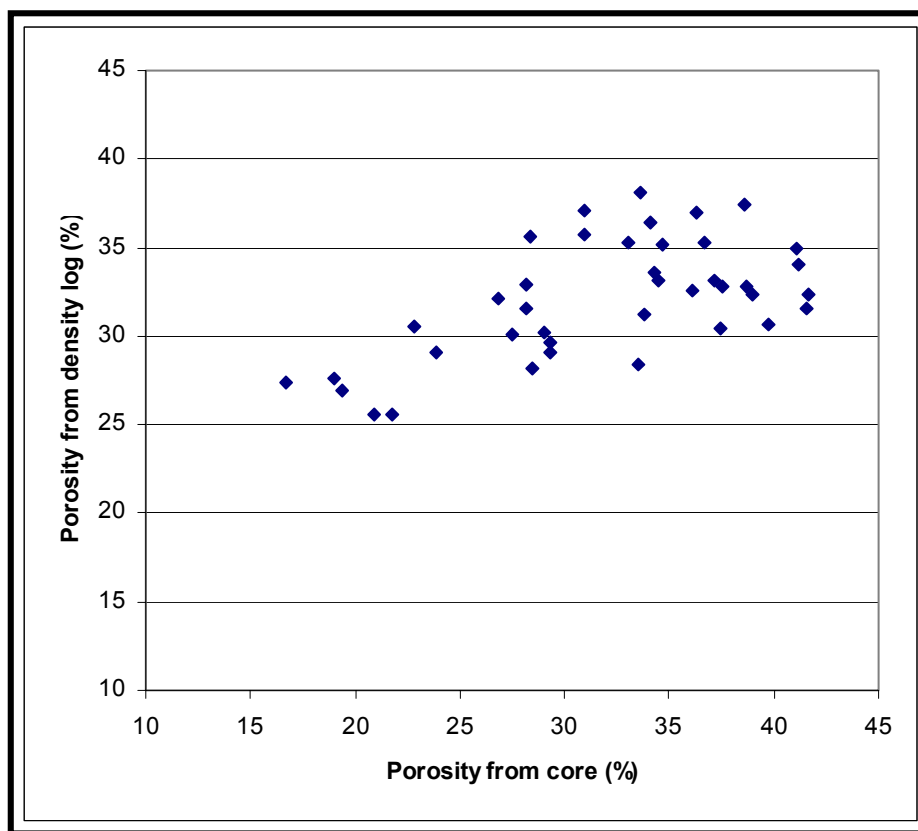


Figure 24-Correlation between porosity values from cores and from logs.

In order to simplify the model we took an average value for each interval with the same facies. In order to determine permeability values, we built a porosity-versus-permeability plot based on core data (figure 25).

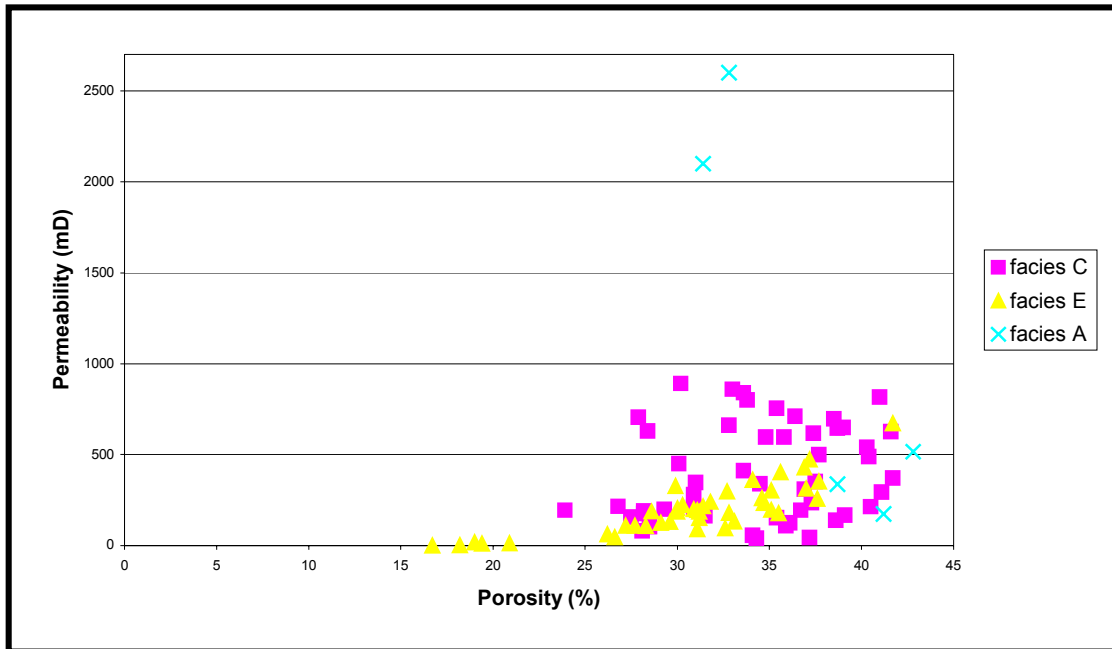


Figure 25-Plot showing petrophysical properties of facies A, C and E.

Permeability and porosity are well correlated for facies E but the relationship is less obvious for facies C and A. We decided to take a value of 2000 mD for all the intervals with facies A. For facies C and E, we used the following type of relationship:

$$\phi = a \log K + b$$

Finally we obtained the results displayed in table 4.

Table 4. Location of facies with associated porosity and permeability values.

Well	Depth (ft TVD)	Facies	Porosity (%)	Permeability (mD)		Well	Depth (ft TVD)	Facies	Porosity (%)	Permeability (mD)		
A-2	9800-9808	E	30	100	E:45%	A-7st	9633-9652	E	29	80	E:37%	
	9808-9827	E	28	70	C:46%		9652-9669	C	31	250	C:63%	
	9827-9848	C	30	200	A:9%		9669-9682	E	28	70		
	9848-9868	C	32	280			9682-9714	C	34	350		
	9868-9878	C	37	500			9714-9743	C	32	280		
	9878-9887	C	35	350		9743-9756	E	30	100			
	9887-9895	A	41	2000		A-8	10303-10315	E	27	50	E:48%	
	9895-9898	C	32	280			10315-10320	C	31	250	C:52%	
	9898-9904	A	40	2000			10320-10321	E	28	70		
	9904-9918	E	28	70			10321-10329	C	31	250		
	9918-9922	C	32	280			10329-10333	C	38	650		
	9922-9927	E	26	40		10333-10343	C	33	300			
	9927-9936	E	29	80		10343-10355	E	27	50			
	9936-9941	C	29	150		A-10	9547-9589	E			E:86%	
	9941-9947	E	26	40			9589-9596	C			C:14%	
9947-9955	E	28	70		A-11	9612-9628	E	27	50	E:58%		
1	9687-9693	C	26	100		E:11%	9628-9639	C	31	250	C:42%	
	9693-9697	E	24	30		C:76%	9639-9654	E	29	80		
	9697-9709	C	31	250		A:13%	9654-9665	E	27	50		
	9709-9713	E	26	40			9665-9673	C	31	250		
	9713-9719	C	37	500		9673-9684	C	33	300			
	9719-9722	C	35	350		A-12	10083-10086	E			E:66%	
	9722-9725	A	39	2000			10086-10098	C	37	500	C:34%	
	9725-9729	C	38	650			10098-10109	C	32	280		
	9729-9735	A	42	2000			10109-10165	E				
	9735-9751	C	39	750		10165-10172	C					
	9751-9759	C	37	500		A-12st	10074-10079	C			E:55%	
	A-3	10139-10147	E	28	70		E:57%	10079-10122	E			C:45%
		10147-10169	C	29	150		C:43%	10122-10129	C			
		10169-10176	E	27	50			10129-10144	E			
		10176-10182	C	33	300			10144-10179	C			
10182-10190		E	29	80		10179-10203	E					
10190-10212		C	35	350		A-25	9656-9667	C	43	800	E:37%	
10212-10249		C	32	280			9667-9684	E	31	130	C:56%	
10249-10275		C	29	150			9684-9687	C	40	650	A:7%	
10275-10283	E	27	50		9687-9693		E	29	80			
10283-10285	C	32	280		9693-9697		C	36	350			
A-5	9531-9533	C	32	280	E:65%		9697-9705	E	32	160		
	9533-9541	E	30	100	C:35%		9705-9710	C	37	500		
	9541-9544	E	36	400			9710-9713	E	32	160		
	9544-9557	E	30	100			9713-9719	C	36	350		
	9557-9564	C	28	150			9719-9724	E	32	160		
9564-9568	C	33	300		9724-9732		C	39	650			
A-7	9636-9655	E	31	130	E:48%		9732-9739	C	42	800		
	9655-9660	C	33	300	C:52%	9739-9745	C	38	500			
	9660-9668	E	28	70		9745-9750	A	38	2000			
	9668-9674	C	31	250		9750-9754	C	42	800			
	9674-9691	E	28	70		9754-9760	C	37	500			
	9691-9705	C	34	350		9760-9763	A	41	2000			
	9705-9720	C	37	500		9763-9770	E	28	70			
	9720-9746	C	33	300		9770-9779	C	35	300			
	9746-9756	E	31	130								
	9756-9763	E	32	160								

All these data were used for populating the 8 Sand reservoir model.

CHAPTER IV

RESULTS

Location of the depositional environment

The study of core pictures and log responses of the 8 Sand reservoir suggested that the facies encountered corresponded to mid-fan deposits. These mid-fan facies are mainly composed of levee, overbank and channel deposits. Figure 26 shows the theoretical location of such a depositional environment.

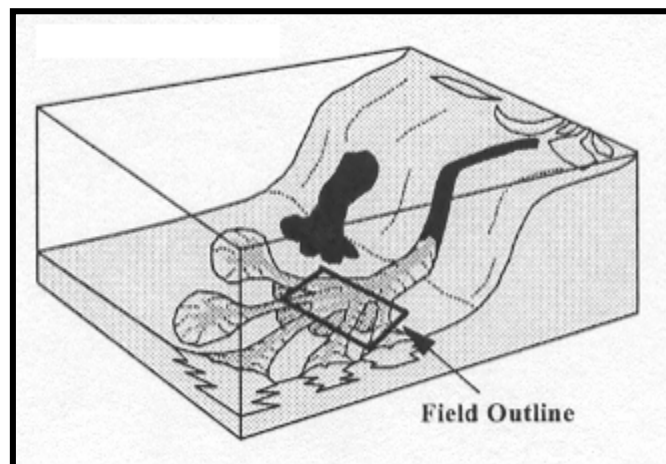


Figure 26-Diagram showing the depositional environment of the 8 Sand reservoir (modified from Davies et al., 1999).

This diagram may not be the exact representation of the depositional environment since we did not figure out how extended were the channel facies in the zone. This sketch represents the turbidite system at a given time, but the 8 Sand reservoir is likely to contain several stacked systems deriving from the lateral migration of a channel system.

Map of the top of the 8 Sand reservoir

The top of the 8 Sand reservoir was picked by S. Lalande on seismic sections. Check-shots performed in the wells were used to convert the time map into a depth map (figure 27). The modeling of this map was performed using Isatis® software. A collocated co-kriging was used to simulate this map (Lalande, 2002). The modeling could not be run to the south of the major fault because no well was drilled in this portion of the field and the seismic quality was very low. Discrepancies would have been dramatically increased in this zone. This map shows that the 8 Sand formation dips northward, which is probably due to the intrusion of a salt dome in the southern area. The modeled area represents the upthrown part of the faulted system.

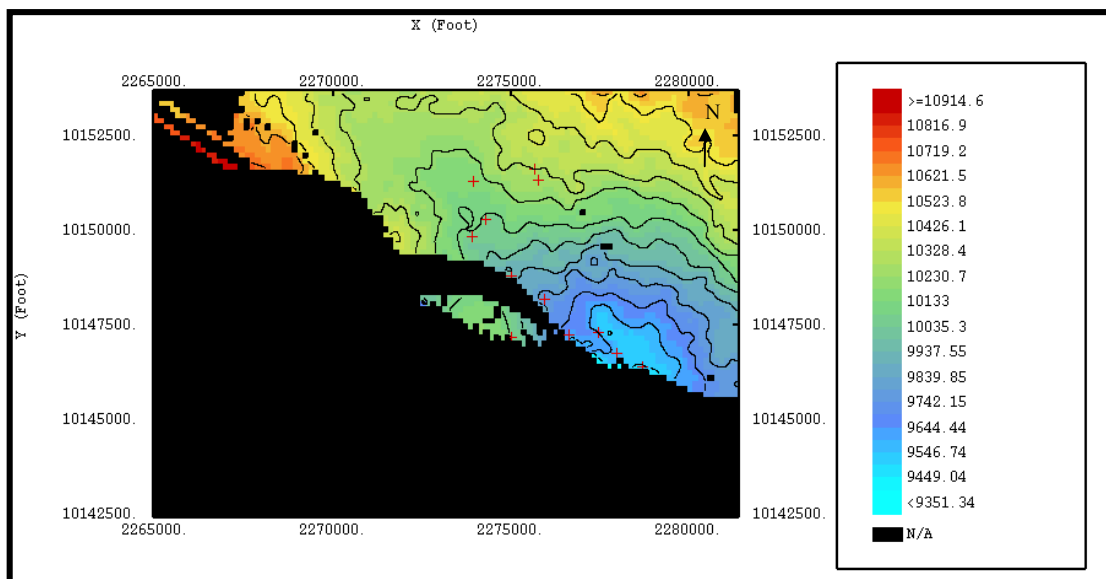


Figure 27-Map of the top of the 8 Sand reservoir. Red crosses indicate well locations. Depth is in feet (from Lalande, 2002).

Gross thickness map

To generate the structure map, a collocated cokriging was run, taking into account seismic and well data (Lalande, 2002). A time-to-depth conversion was performed using check-shot data (figure 28).

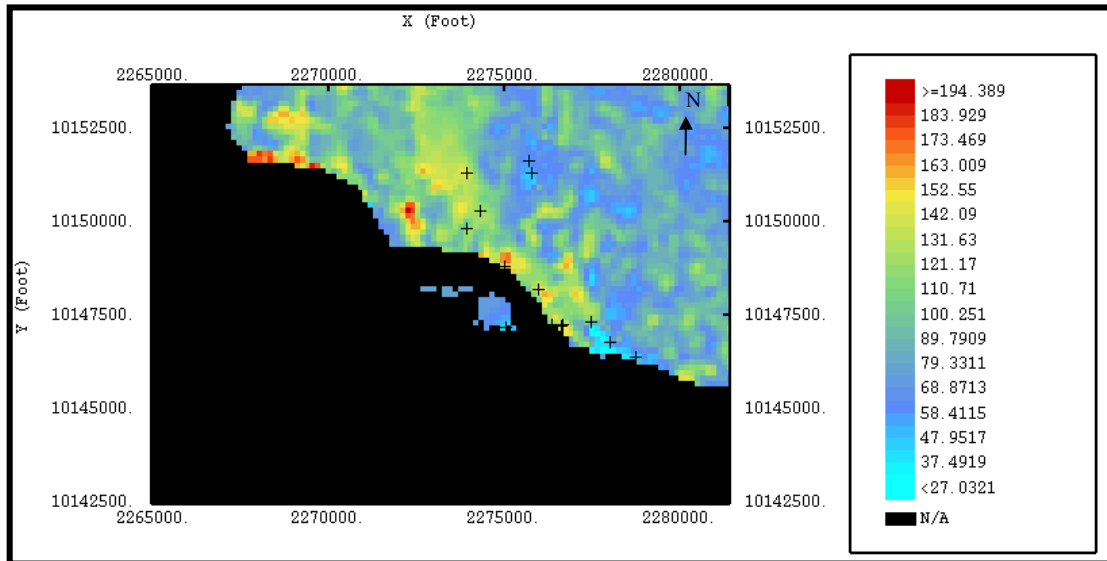


Figure 28-Gross thickness map. Black crosses indicate well locations. Thicknesses are in feet (from Lalande, 2002).

The reservoir gross thickness is relatively heterogeneous and presents some trends that may be linked to sedimentary bodies such as channel deposits.

Net thickness map

Once all the net thickness values were available, the next step consisted in building a net thickness map of this reservoir, which would give a good idea of the 8 Sand reservoir quality. S. Lalande ran the main part of this modeling. In order to take into account the spatial variability of this parameter, it was necessary to introduce a secondary variable that would constrain the modeling of the 8 Sand thickness.

In this objective, S. Lalande studied different seismic attributes and she found a correlation between the half-energy time seismic attribute and the net thickness of the reservoir at the location of the wells (Lalande, 2002). Figure 29 shows the correlation between thickness and this seismic attribute.

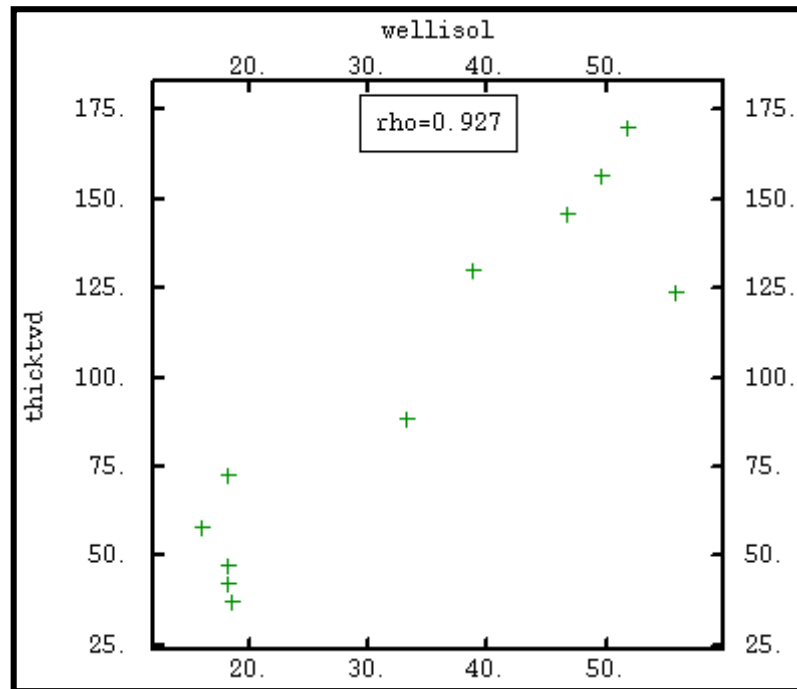


Figure 29-Correlation between half-energy time and reservoir thickness (from Lalande, 2002).

Thus a modeling was run, based on the log data and the spatial variability of this seismic attribute in the 8 Sand reservoir, represented by variograms in several directions (figure 30).

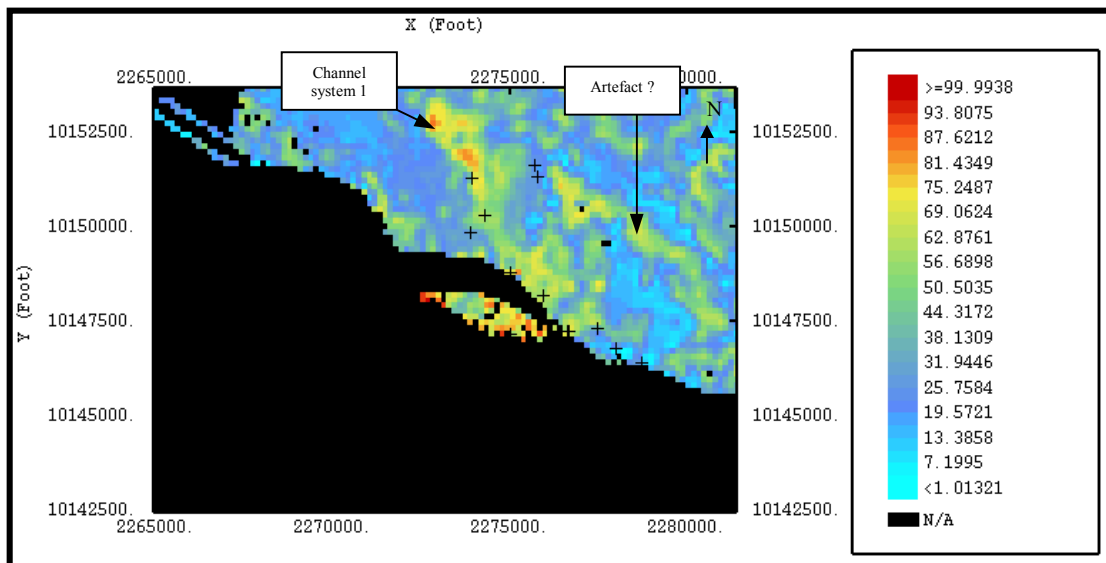


Figure 30-Net thickness map. Black crosses indicate well locations. Thicknesses are in feet (from Lalande, 2002).

We can see that the thickest parts of the 8 Sand reservoir form elongated shapes that have a North West-South East trend, which is in agreement with the direction of the turbidite systems in this zone. The turbidite flow direction was probably influenced by the presence of a salt dome in the southern area of the Green Canyon 18 field. These thicker zones are likely to correspond to channel paths. There seem to be two main channel systems that probably did not work simultaneously. The eastern system is less developed than the other one, maybe because of erosion or reworking by currents. The elongated body in the eastern part of the map is probably only an artefact because modeling was only constrained by half-energy seismic attribute in this zone. We also noticed that reservoir thickness gets lower northward, which is not consistent with the current structure of the area. Salt tectonics has probably tilted the turbidite deposits by lifting the structurally lower parts of the 8 Sand formation.

Well correlations

Correlation between wells led us to obtain three cross sections. These cross-sections only represent one of the possible interpretations that can be performed from our dataset. A lot of uncertainties still remain about the channel location and the relationship between the bodies A and B. Amplitude map shows that there is an unconformity at the boundary between the two bodies, which may be related to a facies change. In some seismic cross-sections, body A seems to overlap body A. But this feature could not be checked in all the cross-sections. We tried to focus on the continuity of the reflectors inside the reservoir but it was very difficult to draw conclusions, due to the low quality of the seismic data (Lalande, 2002). We assumed that channels presented shingled stacking, but we could not figure out how extended were the channel deposits. The only information came from well A-2 in which we observed a 8 feet thick channel deposit. This confirmed that channel stacking was not vertical.

The first cross section (figure 31) was performed in the North West-South East direction and includes the discontinuity between the two bodies A and B. This contact could not be investigated thus its location on the cross-section was purely assumed. The contact is somewhere between well A-2 and 1, but we did not figure out if this contact acts as a barrier for fluid flow with the presence of shale layers.

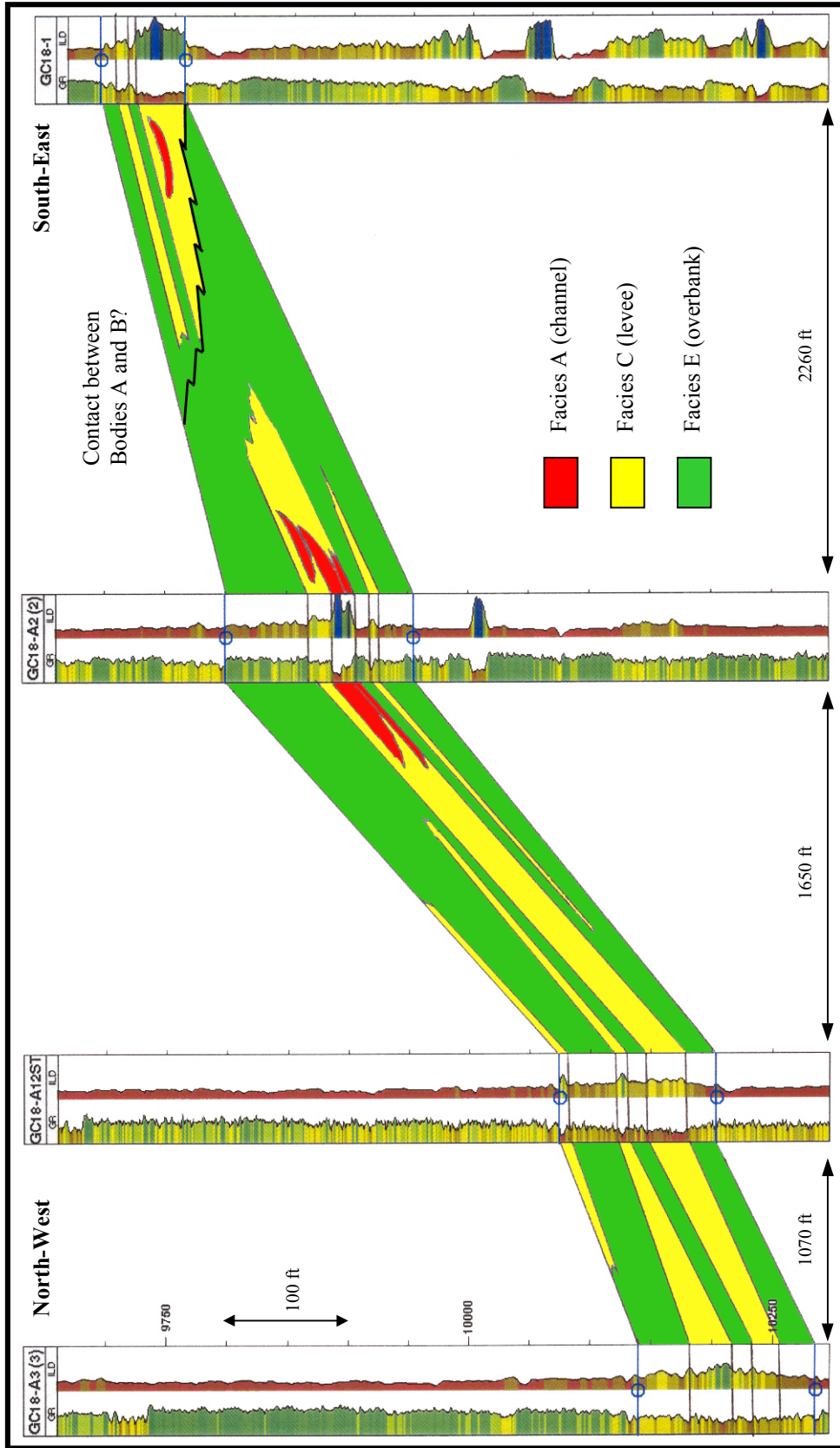


Figure 31-Cross-section 1 from well correlation. Its location is indicated in figure 29.

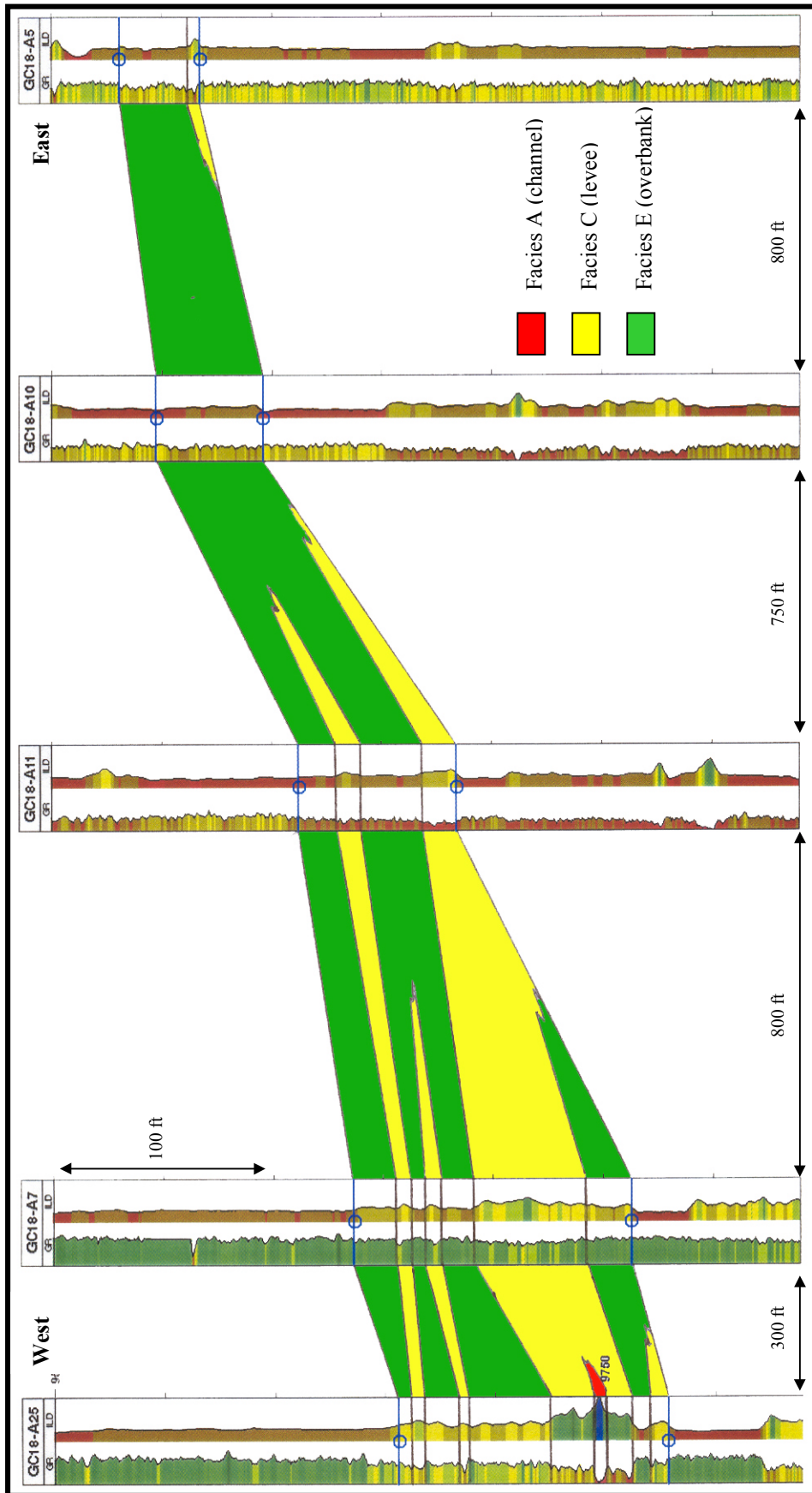


Figure 32-Cross-section 2 from well correlation. Its location is indicated in figure 33.

The second cross-section (figure 32) has a West-East trend and represents a lower-quality part of the 8 Sand reservoir. It is obvious that reservoir quality gets poorer eastward since the deposits are further from channel path. It confirmed that body A does not contain facies as good as in body B, maybe because it was partially eroded by overlying formations. There is no evidence of channel deposits. Well A-25 was assumed to be close to channel edges. Figure 33 shows the location of these cross-sections.

The third cross-section (figure 34) is perpendicular to the channel system path. Wells A-12 and A-12st were drilled in body B while well A-8 crossed body A. Log response is better in A-12st than in A-12 thus we inferred that channel deposits were located to the East of A-12st. Contact between the two bodies could not be investigated so a lot of uncertainties remain in this zone.

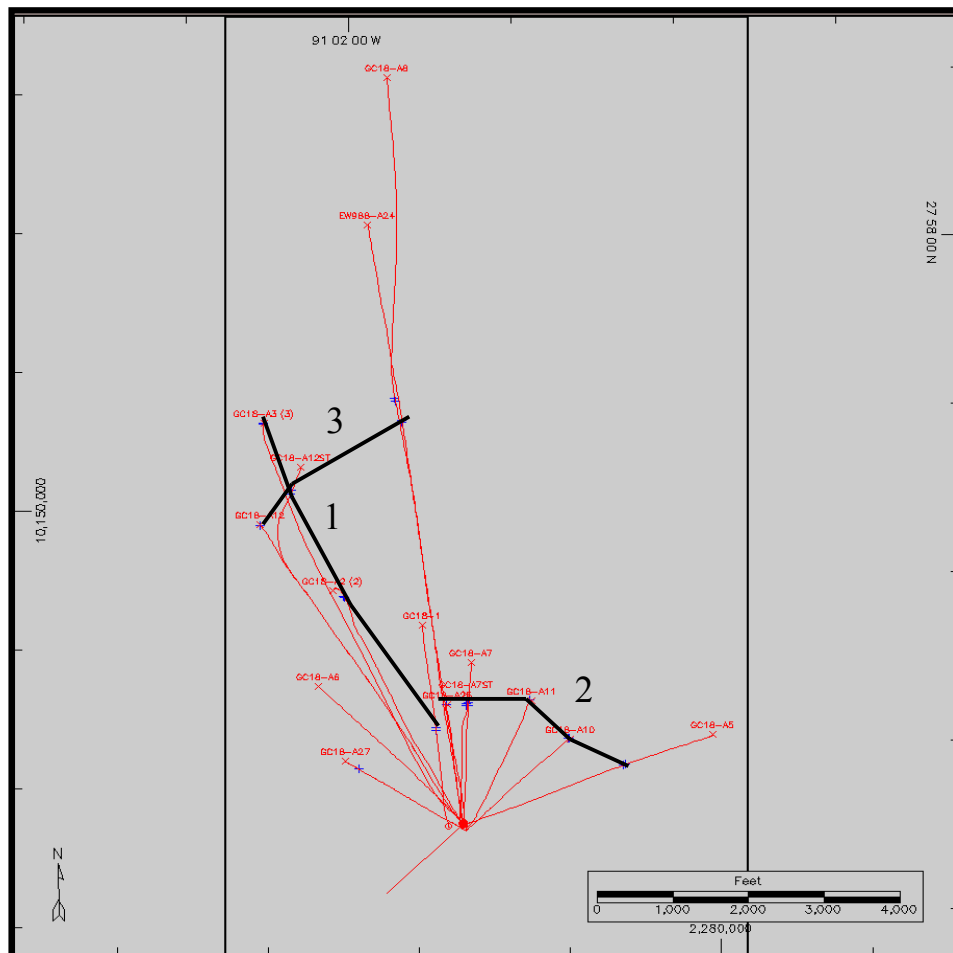


Figure 33-Location of the three cross-sections.

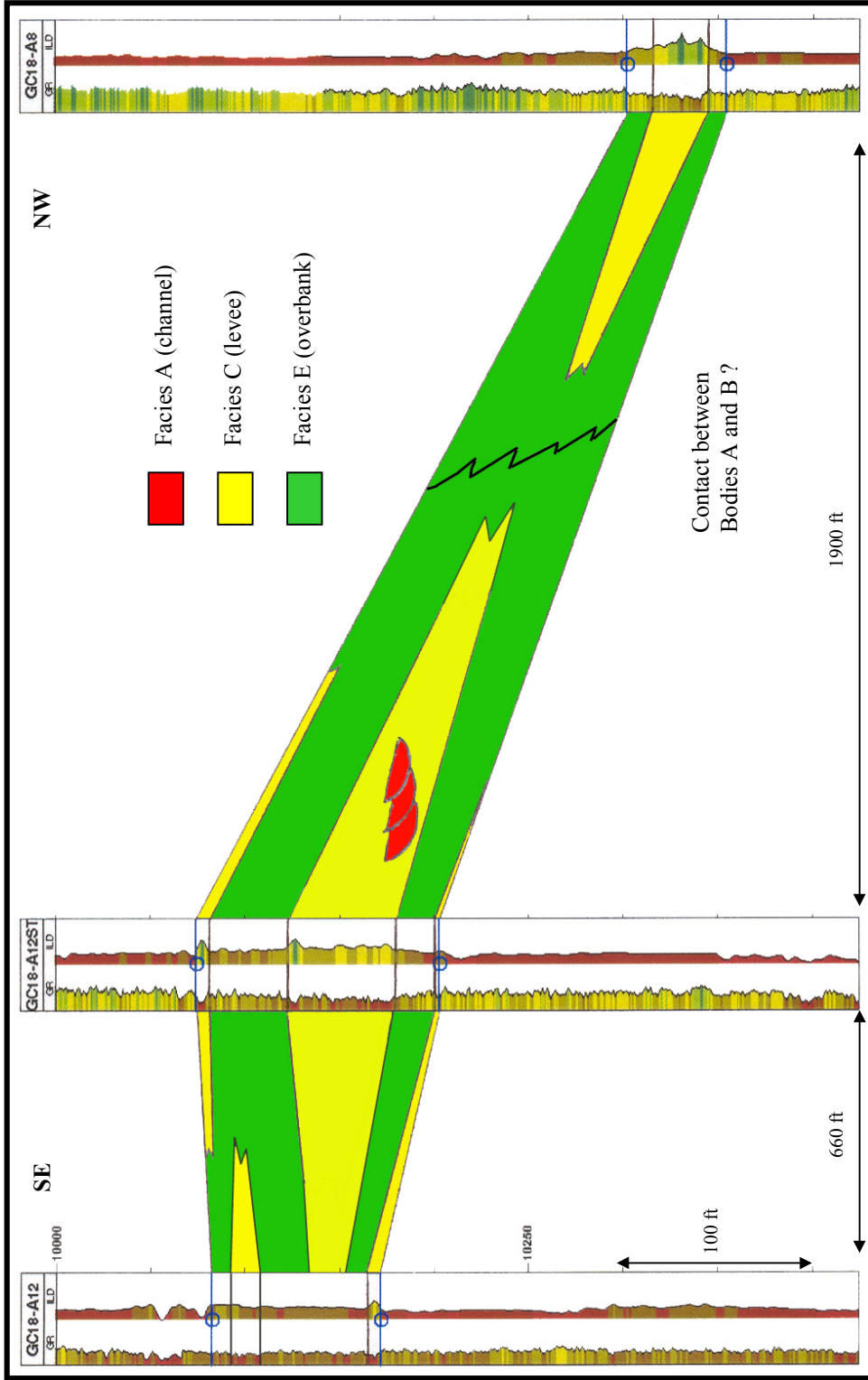


Figure 34-Cross-section 3 from well correlation. Its location is indicated in figure 30. Channels may not be at the right scale

3-D reservoir model

The final step consisted in building a reservoir model with the facies, porosity and permeability values. Seismic attributes could not be used because seismic resolution is not high enough to account for variability inside a 100 ft-thick reservoir. Thus a truncated gaussian simulation, based on facies percentages, was performed to propagate the values available at the well locations. The area was divided into 3 distinct zones in which three independent simulations were performed (Lalande, 2002). The software used for this modeling did not allow taking into account with precision the 8 Sand reservoir shape, but the model obtained gives a good idea of the internal organization of the reservoir.

Figure 35 shows a view of this model, with facies A, C and E populating the reservoir. We can see the shape of the channel system that constitutes the main part of body B (western part). The channel path is curved in this zone, which is probably induced by a topographic high due to salt tectonics. In this model there is no channel deposit in the eastern part of the reservoir, but uncertainties are large in this area. This 3-D model needs to be upscaled before running a reservoir simulation. Later on porosity and permeability maps will be performed, based on the results in table 3.

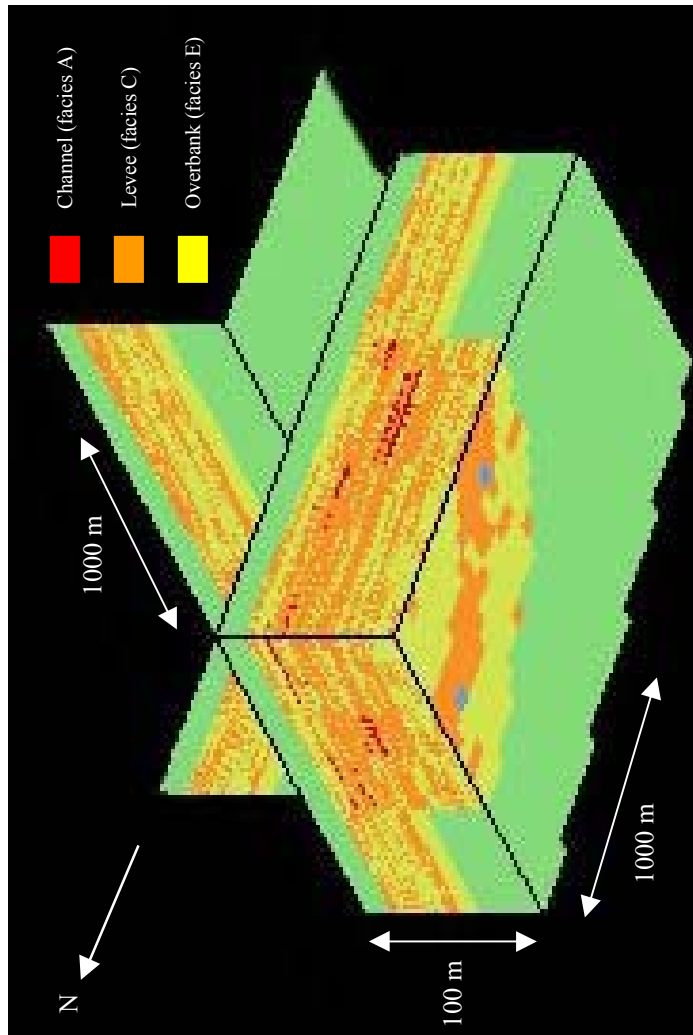


Figure 34-Reservoir model showing the facies repartition within the 8 Sand reservoir (from LaInde, 2002).

CHAPTER V

DISCUSSION

Uncertainties about reservoir shape

The main uncertainties concern the spatial extension of the 8 Sand reservoir. The low quality and the limited extent of seismic sections did not allow S. Lalande determining the limits of the reservoir. Most of the wells are concentrated in the same part of the field, which prevented from characterizing with precision the outer parts of the reservoir. The thickness map may be an indicator of the areal extent of this reservoir. It is reasonable to think that both structural and stratigraphic closure determine the extension of the 8 Sand reservoir. The stratigraphic closure should be done by hemipelagic shale that from the “background” of the sedimentation in the basin. Salt diapirs are also likely to border the reservoir, especially in the southern part of the area. Communication with upper and lower reservoirs could not be demonstrated. Well test data showed that the North West-south East main fault should be a sealing boundary. The lack of data in the southern part of the reservoir and the bad quality of seismic data prevented us from investigating this part of the reservoir.

Continuity inside the reservoir

Previous studies pointed out the existence of two main bodies in the 8 Sand reservoir: they are called 8a and 8b. A-2, A-3 and A-12 are the wells that cross the 8b part of the 8 Sand reservoir, which indicates that this body is located in the northern-west part of the Green Canyon field. Figure 27 shows a discontinuity between the two major sand accumulations, which is likely to be the boundary between the two bodies. Seismic sections tend to show that body A overlies body B, but the poor quality of the seismic signal in this area did not permit to be affirmative on this point. Some pressure and production data were available for the part b of the 8 Sand, but we

did not figure out whether the two sand bodies were well connected or not. The origin of these two bodies remains unclear. They may correspond to two channel systems that were active simultaneously. But the second channel system might have been active after the first one, eroding or not a part of the channel fill that had been deposited previously. Interaction between the different channel systems is a key-point because it defines how the two bodies are connected between each other. Some previous studies concluded that they should be some communication between the two bodies. We also noticed that body A might have been partially eroded after its deposition, which could explain the bad seismic response. There is no evidence of channel deposits in this area. Boundaries between levee and overbank deposits are not likely to represent barriers for fluid flow because the change of facies is usually progressive. Channel width is also misunderstood, but the channels are probably several hundred feet wide. The associated levees and overbank should be more than one thousand feet wide, but this is only an order of magnitude.

Recommendations for future 8 Sand reservoir simulation

The 8 Sand reservoir study led to several conclusions about the way of running a future reservoir simulation.

First the channel locations should be taken into account during history matching. The log and seismic data did not allow us figuring out how extended was this facies.

Log data confirmed that there is a large aquifer at about 10350 feet. It confirmed that this active aquifer is likely to represent a good pressure support during reservoir production.

The kv/kh ratio should be low enough to take into account the laminated nature of sediments in the 8 Sand reservoir. This value should be less than 0,05.

This reservoir is not fractured, which could prevent early water and gas breakthrough during production. The main southern fault is assumed to be a sealing fault, according to well test results.

CHAPTER VI

CONCLUSIONS

Analysis of core and well log data in the Green Canyon 18 field, Gulf of Mexico, allowed characterizing the Upper Pliocene 8 Sand reservoir. It was deposited in one of the mini-basins that were created by salt tectonics. This reservoir is made of fine-grained turbidite deposits that are mainly composed of alternating sand/silt and shale layers. The major part of the facies could be associated with levee and overbank deposits, with some channel deposits deriving from narrow, meandering and laterally migrating turbidite channels fed by shelf material. Then this formation was probably tilted and deformed by fault and salt tectonics, as it is suggested by the presence of a major extensive fault in the southern part of the field and the discrepancies between current structure and reservoir thickness.

The high porosity and horizontal permeability values measured in core data, at least in facies A and C, are mainly due to the absence of diagenetic features in these unconsolidated sediments, and thus mainly depend on the depositional conditions of the turbidite currents. Two channel systems were probably active at different times, and one of them was assumed to having been eroded by new turbidity currents later on. The best facies are located in body B, with a presumed shingled stacking of channels. Cross-sections built from well correlation show that facies are likely to be laterally continuous, even if interactions between the two bodies could not be investigated. All this information will result in the building of a 3-D model of the 8 Sand reservoir.

Large uncertainties still remain in the reservoir geological description, due to the lack of data describing the 8 Sand reservoir. Nevertheless several recommendations could be raised for a future reservoir simulation. One of the most important is the low kv/kh ratio resulting from the laminated structure of sediments. No thick shale layer could be highlighted in the reservoir, but some hemipelagic shales might be present in the reservoir.

REFERENCES CITED

- Beard, D. C., and P. K. Weyl, 1973, Influence of texture on porosity and permeability of unconsolidated sand: AAPG Bulletin, v. 57, p. 349-369.
- Bouma, A. H., W. R. Normark, and N. E. Barnes, eds., 1985a, Submarine fans and related turbidite systems: New-York, Springer-Verlag, 351 p.
- Bouma, A. H., et al., 1985b, Mississippi Fan : Leg 96 program and principal results, *in* A. H. Bouma, W. R. Normark, and N. E. Barnes, eds., 1985a, Submarine fans and related turbidite systems: New-York, Springer-Verlag, p. 247-252.
- Bouma, A. H., C. E. Stelling, and J. M. Coleman, 1985c, Mississippi Fan, Gulf of Mexico, *in* A. H. Bouma, W. R. Normark, and N. E. Barnes, eds., 1985a, Submarine fans and related turbidite systems: New-York, Springer-Verlag, p. 143-150.
- Bouma, A. H., and H. deV. Wickens, 1994, Tanqua Karoo, ancient analog for fine-grained submarine fans, *in* P. Weimer, A. H. Bouma, and B. F. Perkins, eds., Submarine fans and turbidite systems: sequence stratigraphy, reservoir architecture and production characteristics; Gulf of Mexico and international: Gulf Coast Section SEPM 15th Annual Research Conference Proceedings, p. 23-34.
- Bouma, A. H., G. H. Lee, O. van Antwerpen, and T. C. Cook, 1995a, Channel complex architecture of fine-grained submarine fans at the base-of-slope: Gulf Coast Association of Geological Societies Transactions, v. 65, p. 65-70.
- Bouma, A. H., H. D. Wickens, and J. M. Coleman, 1995b, Architectural characteristics of fine-grained submarine fans: a model applicable to the Gulf of Mexico: Gulf Coast Association of Geological Societies Transactions, v. 65, p. 71-75.
- Bouma A. H., 2000, Fine-grained, mud-rich turbidite systems: model and comparison with coarse-grained, sand-rich systems, *in* A. H. Bouma and C. G. Stone, eds., Fine-grained turbidite systems, AAPG Memoir 72/SEPM Special Publication 68, p. 9-20.
- Brenchley, P. J., and G. Newall, 1977, The significance of contorted bedding in the Upper Ordovician sediments of the Oslo region, Norway: Journal of Sedimentary Petrology, v. 47, p. 819-833.
- Brinkmann, P. E., G. J. Barbler, and W. Rodriguez, 1985, Design and installation of a 20-slot template in the Gulf of Mexico in 760 ft of water: paper SPE 14579, presented at the 1985 OTC, Houston, 6-9 May, p. 99-103.
- Damuth, J. E., R. D. Flood, R. O. Kowsmann, R. H. Belderson, and M. A. Goriniet, 1988, Anatomy and growth pattern of Amazon deep-sea fan as revealed by long-

range side-scan sonar (GLORIA) and high-resolution seismic studies: AAPG Bulletin, v. 72, p. 885-911.

Darling, H. L., and R. M. Sneider, 1992, Production of low resistivity, low-contrast reservoirs, offshore Gulf of Mexico basin: Gulf Coast Association of Geological Societies Transactions, v. 42, p. 73-88.

Davies, D. K., P. S. Hara, and J. J. Mondragon, 1999, Geometry, internal heterogeneity and permeability distribution in turbidite reservoirs, Pliocene California: paper SPE 56819, presented at the 1999 SPE Annual Technical Conference and Exhibition, Houston, 3-6 October.

Dunham, L., 1993, Personal communication.

Lalande, S., 2002, Characterization of a thin-bedded reservoir in the Gulf of Mexico: an integrated approach: Master's thesis, Texas A&M University, College Station, Texas, 60 p.

McPherson, J. G., 1982, Personal communication.

Menard, H. W., 1955, Deep-sea channels, topography, and sedimentation: AAPG Bulletin, v. 39, p. 236-255.

Mutti, E., and W. R. Normark, 1987, Comparing examples of modern and ancient turbidite systems: problems and concepts, *in* J. K. Leggett and G. G. Zuffa, eds., Marine clastic geometry: concepts and case studies: London, Graham and Troutman, p. 1-38.

Mutti, E., and W. R. Normark, 1991, An integrated approach to the study of turbidite systems, *in* P. Weimer, and M. H. Link, eds., Seismic facies and sedimentary processes of submarine fans and turbidite systems: New-York, Springer-Verlag, p. 75-106.

Ostermeier, R. M., 1993, Deepwater Gulf of Mexico turbidites: compaction effects on porosity and permeability: paper SPE 26468, presented at the 1993 Annual Technical Conference and Exhibition, Houston, 3-6 October, p. 539-551.

Posamentier, H. W., M. T. Jervey, and P. R. Vail, 1988, Eustatic controls on clastic deposition 1-conceptual framework, *in* C. K. Wilgus, B. S. Hasting, C. G. S. C.Kendall, H. W. Posamentier, C. A. Ross, and J. C. Van Wagoner, eds., Sea level changes: an integrated approach: SEPM Special Publication 42, p. 109-124.

Reading, H. G., and M. Richards, 1994, Turbidite systems in deep-water basin margins classified by grain size and feeder system: AAPG Bulletin, v. 78, p. 792-822.

Reedy, G. K., and C. F. Pepper, 1996, Analysis of finely laminated deep marine turbidites: integration of core and log data yields a novel interpretation model: paper SPE 36506, presented at the 1996 Annual Technical Conference and Exhibition, Denver, Colorado, 6-9 October, p. 119-127.

Reineck, H. E., and I. B. Singh, 1973, Depositional sedimentary environments: New-York, Springer-Verlag, 439 p.

Stelting, C. E., A. H. Bouma, and C. G. Stone, 2000, Fine-grained turbidite systems: overview, *in* A. H. Bouma and C. G. Stone, eds., fine-grained turbidite systems, AAPG Memoir 72/SEPM Special Publication 68, p. 1-8.

Weimer, P., P. Varnai, F. M. Budhijanto, Z. M. Acosta, and R. E. Martinez, 1998, Sequence stratigraphy of Pliocene and Pleistocene turbidite systems, Northern Green Canyon and Ewing Bank (offshore Louisiana), Northern Gulf of Mexico: AAPG Bulletin, v. 82, p. 918-960.

Williams, L. I., 2000, Personal communication.

VITA

Matthieu Plantevin

Date of birth: March 13, 1976

Education: M.S. Geology, Texas A&M University, 2002
M.S. Reservoir Geoscience and Engineering, IFP School, France, 2002
B.Sc. (engineering degree) Geology, Ecole Nationale Supérieure de Géologie, France, 2000

Experience: January to May 2002-Graduate Assistant Research, Petroleum Engineering Department, Texas A&M University.

January to August 2000- Training period within TOTAL FINA (Paris) with reservoir characterization objective by studying West Africa trend curves.

Summer 1999- Training period within ELF EP (Pau, France) based on the underlining of Low Resistivity Sand type reservoirs (wireline logging studies).

Mailing address: 31, rempart Saint Pierre
71100 Chalon sur Saone
France